理學碩士學位論文

인체 장내 유익균 *Faecalibacterium prausnitzii* 의 당 수송 인산전달계 기능성 연구

Functional dissection of the PTS in beneficial gut bacterium *Faecalibacterium prausnitzii*

2021年 8月

서울大學校 大學院

生命科學部

강드보라

인체 장내 유익균 *Faecalibacterium prausnitzii* 의 당 수송 인산전달계 기능성 연구

指導敎授 石 暎 宰

이 論文을 理學碩士學位論文으로 提出함

2021年 7月

서울大學校 大學院

生命科學部

강드보라

강드보라의 理學碩士學位論文을 認准함

2021年 7月

委 員 長 허 원 기

副委員長 석 영 재

委 員 박 주 홍

Abstract

Deborah Kang

School of Biological Sciences

The Graduate School

Seoul National University

Faecalibacterium prausnitzii is a dominant member of healthy human colon microbiota, regarded as a beneficial gut bacterium due to its ability to produce anti-inflammatory substances. However, little is known about how *F. prausnitzii* utilizes the nutrients present in the human gut, influencing its prevalence in the host intestinal environment. The phosphoenolpyruvate (PEP): carbohydrate phosphotransferase system (PTS) is an efficient nutrient-uptake mechanism widely shared in the bacterial kingdom. In the PTS, the phosphate group donated from PEP is sequentially transferred from the general components, the enzyme I (EI) and HPr, further to the sugar-specific enzyme II (EII) complexes and finally to the incoming sugar. Besides the role in sugar translocation, the phosphorylation-dependent protein-protein interactions of the PTS proteins are known to regulate various cell physiologies critical to cell survival. Previously, 16 genes encoding putative PTS components (2 enzyme I, 2 HPr, and 12 enzyme II components) in *F. prausnitzii* A2-165 were identified. It was further revealed that among the two homologs, only one of the EI is functional. Likewise, only one of the HPr (HPr1) mainly participated in the PEP-dependent phosphotransfer whereas another HPr (HPr2) might play regulatory roles. Regarding the sugar-specific components, I developed an *in vitro* phosphotransferase assay to visualize the presence of PTS membrane compartments in the membranous proteins extracted from *F. prausnitzii* cultured on cognate PTS sugars. Hence, I could determine the functional pairs of the PTS components that participate in the transport of *N*-acetylglucosamine and fructose. Furthermore, the regulatory function of the PTS components was studied by investigating the newly identified interaction between HPr2 and galactose-1-phosphate uridylyltransferase, an enzyme required

for galactose catabolism. Overall, I could uncover the involvement of the PTS components in *F. prausnitzii* in the uptake of carbohydrates commonly present in the human gut and suggest that the dissection of the functional PTS in *F. prausnitzii* may help to understand how this vulnerable species outcompetes other bacterial species in the human intestine.

Keywords:

***Faecalibacterium prausnitzii*, gut bacteria, phosphoenolpyruvate: carbohydrate phosphotransferase system, *N*-acetylglucosamine PTS, fructose PTS, galactose-1-phosphate uridylyltransferase, bacterial physiology**

Student Number: 2019-24211

Table of Contents

I. Introduction

1. *Faecalibacterium prausnitzii*

1.1 Overview of *F. prausnitzii*

Firmicutes, together with Bacteroidetes, consists of over 90% of the human gut microbiome. Among these Firmicutes, *Clostridium* cluster XIVa and IV make up 10 to 40% of the total microbiome (Guo *et al*., 2020). Belonging to *Clostridium* cluster IV, *F. prausnitzii* is one of the most abundant bacterial species residing in the large intestines of humans, accounting for 5 to 15% of the total bacterial population (Zoetendal *et al*., 2008; Miquel *et al*., 2015). The gram-positive bacteria are extremely sensitive to oxygen, yet the oxygen sensitivity differs between its two phylogroups. Although some discrepancies exist between previous data, the two major phylogroups have been proposed according to 16S rRNA gene sequences. Generally, phylogroup II is thought to be more resistant to oxidative stress as it was reported that strain A2-165 possess an extracellular electron shuttle, using very low oxygen concentrations to regenerate NADH (Khan *et al*., 2012). Regardless of its phylogroups, the bacterium is rod-shaped, non-sporeforming, and non-motile. With the genomic DNA G+C content 55.7 to 63.0%, the genome size of *F. prausnitzii* is mostly 2.68 to 3.32 Mb (Fitzgerald *et al*., 2018).

1.2 Clinical importance of *F. prausnitzii*

F. prausnitzii is one of the most abundant species among over 1000 bacterial species

constituting the human intestinal microbiota of healthy adults (Arumugam *et al*., 2011; Zoetendal *et al*., 2008). *F. prausnitzii* is known as a beneficial symbiont since it was found to produce and secrete molecules that benefit the host animal. One of the main beneficial end-products of *F. prausnitzii* fermentation is butyric acid, proven to enhance insulin sensitivity, gut motility, and the tight junction of the intestinal epithelial cells (Flint *et al*., 2012; Tremaroli and Backhed, 2012). The microbial anti-inflammatory molecule (MAM) secreted by *F. prausnitzii* was also recently identified to inactivate the NF-κB pathway, the well-identified inflammation response mechanism in mammal cells, when tested *in vivo* and *in vitro* (Breyner *et al*., 2017; Quevrain *et al*., 2016; Sokol *et al.,* 2008).

At the same time, the bacterium has gained attention when sequencing of 16S rRNA libraries of human fecal DNA revealed that the number of *F. prausnitzii* was negatively correlated to the severity of well-known chronic inflammatory diseases such as Inflammatory Bowel Disease (IBD), accounting for both Crohn's disease (CD) and ulcerative colitis (UC), and type two diabetes (T2D) (Cao *et al*., 2014; Gurung *et al*., 2020; Miquel *et al.,* 2013; Sokol *et al.,* 2008). Furthermore, dysbiosis in the sub-species of *F. prausnitzii* was reported to be related to the progression of atopic dermatitis (AD) (Song *et al.,* 2016). Hence, many published research data have suggested that this genus may play a role as a biomarker for the detection of the occurrence of these illnesses and become promising next-generation probiotics (Foditsch *et al*., 2014; Geirnaert *et al*., 2017; Khan *et al*., 2014; Martín *et al*., 2018). Despite the numerous studies conducted on *F. prausnitzii* of the effect of its metabolites on intestinal cells or its inverse correlation with relevant diseases, the studies that support such clinical importance are surprisingly limited to the confirmation of its growth on several carbon sources available in the gut (Duncan *et*

al., 2002; Lopez-Siles *et al*., 2012; Miquel *et al*., 2014), or its genomic analysis using whole-genome sequencing (Heinken *et al*., 2014; Fitzgerald *et al*., 2018). Moreover, only a few studies have reported the activities of either nutrient transporters or catabolic enzymes encoded by the genes identified in the *F. prausnitzii* genome, which may indicate its ability to colonize and proliferate in the gut (Heinken *et al.,* 2014). Overall, there exists a wide gap between the medical interest and the understood biology of *F. prausnitzii* that needs to be filled.

2. Phosphoenolpyruvate: carbohydrate phosphotransferase system (PTS)

2.1 Overview of the PTS

Many bacteria rely on the phosphoenolpyruvate (PEP): carbohydrate phosphotransferase system (PTS) to efficiently import carbohydrates into cells by the concomitant transfer of phosphate from phosphoenolpyruvate (PEP) to the incoming sugar (Stülke and Hillen, 1998). The PTS consists of two general proteins shared for the transport of all PTS-sugars, the enzyme I (EI) and histidine-containing phosphocarrier protein (HPr), and several sugar-specific enzyme II (EII) complexes. The phosphoryl group is transferred from PEP to EI, HPr, EIIA, and EIIB, which subsequently phosphorylates a PTS sugar during its translocation into the cell through EIIC (Deutscher *et al*., 2014) (Figure 1). Thus, the phosphorylation states of the PTS components are modulated in response to the available carbon source (Deutscher *et al*., 2014), and may indicate the availability of carbohydrates as well as the intracellular energy conditions (Kotrba *et al*., 2001).

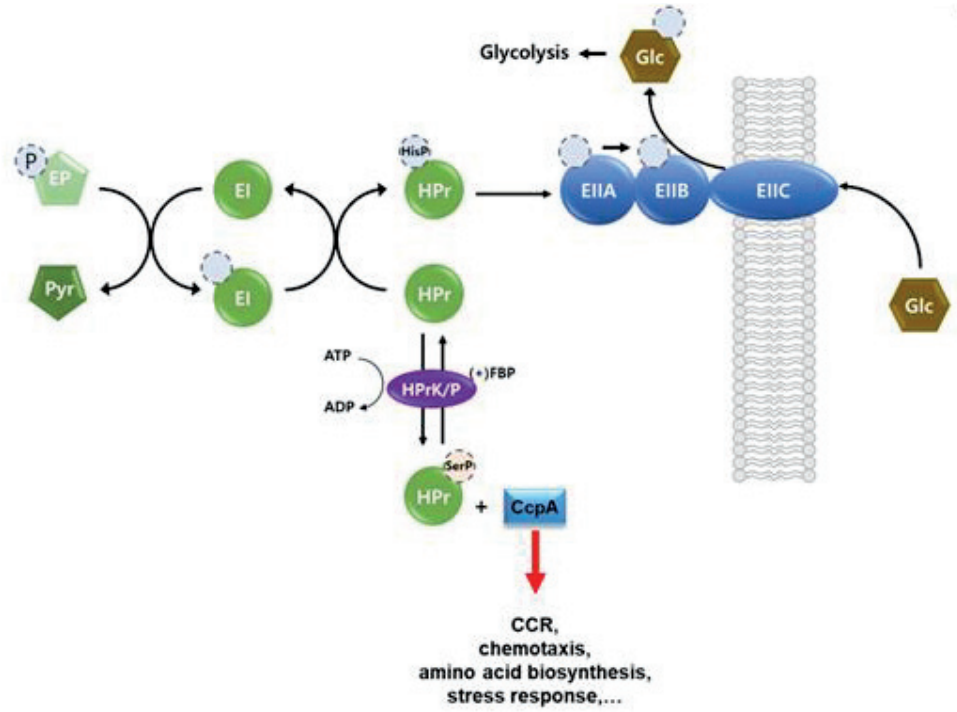

Figure 1. Illustration of the glucose PTS in *Bacillus subtilis*

The phosphorylation cascade initiates with the autophosphorylation of EI by the glycolytic intermediate PEP. EI transfers its phosphoryl group to HPr and phosphoryl relay proceeds sequentially to the membrane-bound carbohydrate-specific EII domains, and finally to the incoming sugar, which is transported across the membrane concomitant with its phosphorylation. HPr can be phosphorylated at two different sites: at Histidine-15 residue via phosphoryl group transfer from EI and at Serine-46 residue via HprK and ATP. The HPr (Ser-P) can act as a cofactor of CcpA and regulate various cell physiologies. CCR; carbon catabolite repression, FBP; Fructose 1,6-bisphosphate, Glc; Glucose, Pyr; pyruvate, PEP; phosphoenolpyruvate.

The PTS components are also important as they play physiological roles by interacting with their cognate partners in a phosphorylation-dependent manner; they were found to regulate glycolysis, gluconeogenesis, stress response, quorum sensing, virulence, and many more in well-studied bacteria such as *Escherichia coli* and *Vibrio cholerae* (Choe et al., 2017; Deutscher et al., 2006; Heo et al., 2019; Kim et al., 2015; Park et al., 2016; Park et al., 2013). Furthermore, in gram-positive bacteria, it is known that the ATP-dependent phosphorylation of HPr on the Ser-46 residue by HPr kinase/phosphatase (HPrK/P) is involved in physiological regulation, such as carbon catabolite repression, amino acid synthesis, and more, by binding to the global transcription regulator catabolite control protein A (CcpA) (Singh et al., 2008). Therefore, a systematic functional analysis of the PTS components is crucial for understanding the basic physiology of any bacterial species.

2.2 Overview of the *F. prausnitzii* A2-165 PTS

A recent study conducted on the identification of the metabolic capabilities of *F. prausnitzii* A2-165 suggested that several carbohydrates could be transported through the PTS (Heinken *et al.*, 2014). However, the PTS genes have not been annotated clearly because the function of these proteins has not been validated. Therefore, by examining the recently updated reference genome of *F. prausnitzii* A2-165 (NCBI PRJNA224116), 16 putative PTS genes among the 2,837 coding genes were identified based on the gene annotations given by the NCBI database (unpublished). The selected genes were compared to the genome of *F. prausnitzii* A2-165 in KEGG (NCBI PRJNA394904) for the verification of their annotations (Table 1). Thereafter, the protein sequences of these genes were aligned to the

Table 1 Putative PTS proteins of *F. prausnitzii* A2-165

NCBI PRJNA224116		KEGG	*Bacillus subtilis* 168 BLASTp hit		Proposed Annotation
Locus	Annotation	Annotation	Protein	Identity (%)	
GXM22_RS00575	PEP-phosphotransferase	PTS system enzyme I (CG447_08375)[a]	PTS enzyme I (*ptsI*)	32	N.F.
GXM22_RS01250	PEP-phosphotransferase	PTS system enzyme I (CG447_07705)	PTS enzyme I (*ptsI*)	42	EI
GXM22_RS01245	HPr	phosphocarrier protein HPr (CG447_07710)	HPr family phosphocarrier protein (*ptsH*)	40	HPr1
GXM22_RS11900	HPr	phosphocarrier protein HPr (CG447_12060)	HPr family phosphocarrier protein (*ptsH*)	44	HPr2, HPrK/P substrate
GXM22_RS01420	PTS glucose transporter subunit IIA	PTS glucose transporter subunit IIA (CG447_07530)	beta-glucoside transporter subunit IIABC (*bglP*)	43	$EIIA^{NAG}$
GXM22_RS00590	PTS transporter subunit EIIC	*N*-acetylglucosamine PTS system EIICB component (CG447_08360)	*N*-acetylglucosamine-specific enzyme IICB component (*nagP*)	41	$EIICB^{NAG}$
GXM22_RS09805	PTS sugar transporter subunit IIA	fructose PTS system EIIABC component (CG447_14155)	fructose-specific enzyme IIABC component (*fruA*)	45	$EIIABC^{Fru}$
GXM22_RS14870	PTS transporter subunit EIIC	maltose/glucose PTS system EIICB component (CG447_09070)	α-glucoside-specific enzyme IICB component (*malP*)	30	Cryptic
GXM22_RS04190	PTS sugar transporter subunit IIA	mannose PTS system EIIA component (CG447_04745)	mannose/fructose/sorbose family IIA component	21[b]	N.F.
GXM22_RS04185	PTS sugar transporter subunit IIB	mannose PTS system EIIB component (CG447_04750)	mannose/fructose/sorbose family IIB component	28	N.F.
GXM22_RS04180	PTS sugar transporter subunit IIC	PTS sugar transporter subunit IIC (CG447_04755)	mannose/fructose/sorbose family IIC component	25	N.F.
GXM22_RS04175	PTS system mannose/fructose/sorbose family transporter subunit IID	fructoselysine/glucoselysine PTS system EIID component (CG447_04760)	mannose/fructose/sorbose family IID component	29[b]	N.F.
GXM22_RS01370	PTS sugar transporter subunit IIA	mannose PTS system EIIA component (CG447_07580)	mannose/fructose/sorbose family IIA component	22[b]	N.F.
GXM22_RS01340	PTS sugar transporter subunit IIB	mannose PTS system EIIB component (CG447_07610)	mannose/fructose/sorbose family IIB component	35	N.F.
GXM22_RS01345	PTS sugar transporter subunit IIC	mannose PTS system EIIC component (CG447_07605)	mannose/fructose/sorbose family IIC component	26	N.F.
GXM22_RS01350	PTS system mannose/fructose/sorbose family transporter subunit IID	fructoselysine/glucoselysine PTS system EIID component (CG447_07600)	mannose/fructose/sorbose family IID component	33	N.F.

[a]Locus tag identified on KEGG database (NCBI PRJNA394904)

[b]Sequence identity obtained through DELTA-BLAST due to no significant similarity using BLASTp.

Abbreviation: N.F., non-functional.

Bacillus subtilis 168 genome (NCBI PRJNA76), whose PTS components have been fully annotated. As a result, two EI homologs (encoded by GXM22_RS00575 and GXM22_RS01250), two HPr homologs (encoded by GXM22_RS01245 and GXM22_RS11900), and five putative sugar-specific enzyme II (EII) complexes consisting of twelve components were identified in the *F. prausnitzii* A2-165 genome (Figure 2 and Table 1). An HPrK/P-encoding gene (GXM22_RS07750) is also present in the *F. prausnitzii* A2-165 genome, similar to that observed in other Gram-positive bacteria.

GXM22_RS01250 and GXM22_RS01245, encoding putative EI and HPr, respectively, are adjacent to each other, while GXM22_RS00575 and GXM22_RS11900 are located separately from other PTS genes in the chromosome. There are two contiguous PTS gene clusters, encoding two different mannose-family EIIs; GXM22_RS04175, RS04180, RS04185, and RS04190 encode EIID, EIIC, EIIB, and EIIA components, while GXM22_RS01340, RS01345, and RS01350 encode EIIB, EIIC, and EIID components, respectively. GXM22_RS01370, encoding a putative mannose-family EIIA component, is located near GXM22_RS01350. However, the genes encoding the *B. subtilis* glucose-specific EIIA homolog (GXM22_RS01420), fructose-specific EIIABC (GXM22_RS09805), and two glucose-family EIICBs (GXM22_RS00590 and RS14870) are scattered over the chromosome.

2.2.1 General components of the PTS

Previously, attempts in our laboratory have revealed several unique features of the PTS in *F. prausnitzii* A2-165, which possesses two copies of each of the general components; the results show that the functionality of the general PTS components

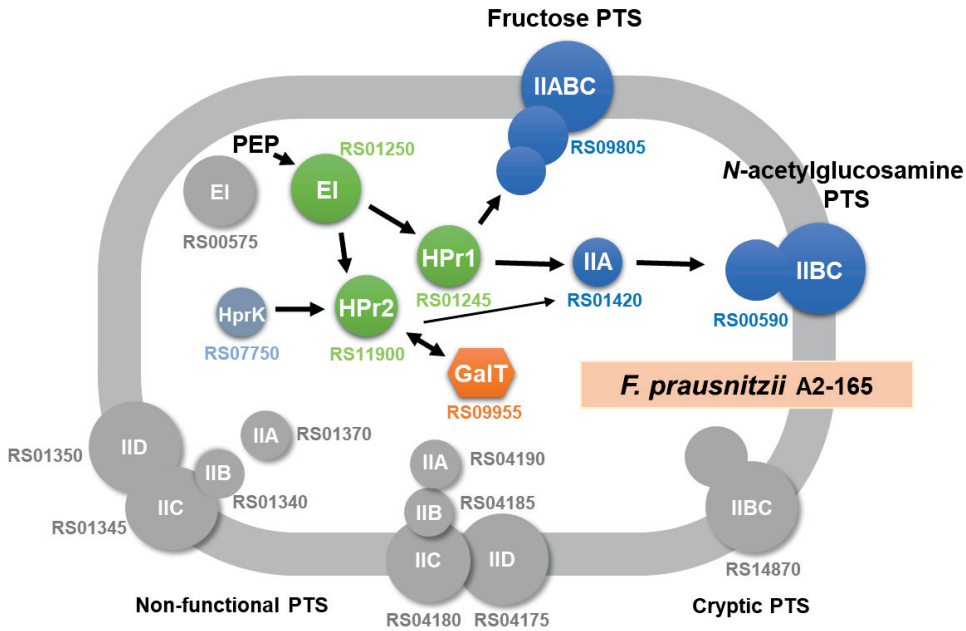

Figure 2. Overview of the PTS in *F. prausnitzii* A2-165

Among the 16 PTS components identified through genomic analysis, EI and HPr1 actively participated in the phosphotransfer reaction to import NAG and fructose translocated through their cognate PTS membrane components. HPr2, which can be phosphorylated by HPrK/P, appears to play regulatory roles different from those played by HPr1, and may possibly regulate GalT. One of the EI homologs and other sugar-specific EIIBC complexes are likely to be non-functional or cryptic.

is different between the two homologs. To verify the activities of the general PTS components of *F. prausnitzii*, *in vitro* phosphorylation assays were performed using two EI homologs and HPr homologs. It is known that a phosphorylated HPr demonstrates higher mobility (phosphorylation-dependent electrophoretic mobility shift, PDEMS) than its unphosphorylated form in native-polyacrylamide gel electrophoresis (PAGE) (Gassner *et al*., 1977; Reizer *et al*., 1983) whereas EIIA usually shows decreased mobility in SDS-PAGE upon phosphorylation (Dörschug *et al.*, 1984; Hogema *et al.*, 1998; Lee *et al.*, 2019). The native-PAGE data showed that neither of the two HPrs, herein referred to as HPr1 (GXM22_RS01245) and HPr2 (GXM22_RS11900), were phosphorylated by GXM22_RS00575-encoded EI, as no PDEMS was detected in the presence of PEP (Figure 3A), indicating that the GXM22_RS00575 gene product was not functional, at least in terms of its phosphotransferase activity. The lack of phosphotransferase activity of the GXM22_RS00575 gene product was also confirmed by the absence of PDEMS of the EIIA encoded by GXM22_RS01420 in SDS-PAGE when incubated with either of the two HPrs and PEP (Data not shown). In contrast, the other EI homolog, encoded by GXM22_RS01250 exhibited phosphotransferase activity, as shown by the PDEMS of both HPr homologs in the presence of PEP (Figure 3B). Despite the absence of phosphotransferase activity of EI (GXM22_RS00575), the amino acid sequences around the His residue responsible for the autophosphorylation by PEP (Alpert *et al.*, 1985) were conserved in both EIs. Hence, the autophosphorylation of EI (GXM22_RS00575) was tested by performing the identical phosphorylation assay with *E. coli* HPr (EcHPr). As a result, the PDEMS of EIIA (GXM22_RS01420) was observed in the reaction with EcHPr and PEP (Data not shown). Therefore, it was concluded that although both EI homologs could be autophosphorylated by PEP,

only the GXM22_RS01250 gene product (hereafter referred to as *ptsI*, encoding EI) participated in the catalysis of PEP-dependent phosphoryl transfer reaction in *F. prausnitzii*.

While only the EI encoded by gene GXM22_RS01250 showed phosphotransferase activity, both HPrs were functional yet displayed a difference in performance. It is known that HPrs of Gram-positive bacteria harbor another phosphorylation site at the Ser-46 residue, whose reaction is catalyzed by ATP-dependent kinase HPrK/P (Deutscher *et al.*, 2006). Interestingly, the two HPr homologs in *F. prausnitzii* A2-165 were distinguishable by the Ser-46 residue, which was only present in HPr2. Therefore, the HPrK/P-dependent phosphorylation of HPr homologs were examined in the presence of ATP. As expected, HPr1 showed no band shift in native-PAGE upon incubation with HPrK/P and ATP (Figure 9A). In contrast, HPr2 was phosphorylated by HPrK/P when ATP was added (Figure 9B, lane 2). Interestingly, the band shift of serine-phosphorylated HPr2 (HPr2[Ser-P]) could be distinguished from that of histidine-phosphorylated HPr2 (HPr2[His-P]) due to the difference in mobility shift demonstrated on the native-PAGE gel (Figure 9B, lanes 1 and 2). According to a previous study (Halbedel and Stülke, 2005), these two phosphorylation reactions are mutually exclusive, because phosphorylation at His-15 residue diminishes the affinity between HPrK/P and its protein substrate (Wang *et al.*, 2000; Fieulaine *et al*., 2002; Deutscher *et al*., 2006). Surprisingly, incubation of HPr2 with HPrK/P and EI in the presence of PEP and ATP led to the formation of a doubly phosphorylated form, HPr2(His-P/Ser-P), with a significant decrease in HPr2(His-P) in comparison to HPr2(Ser-P), thereby implying that under the employed experimental conditions, serine phosphorylation by HPrK/P constitutes the major phosphorylation event in HPr2 (Figure 9B, lane 3).

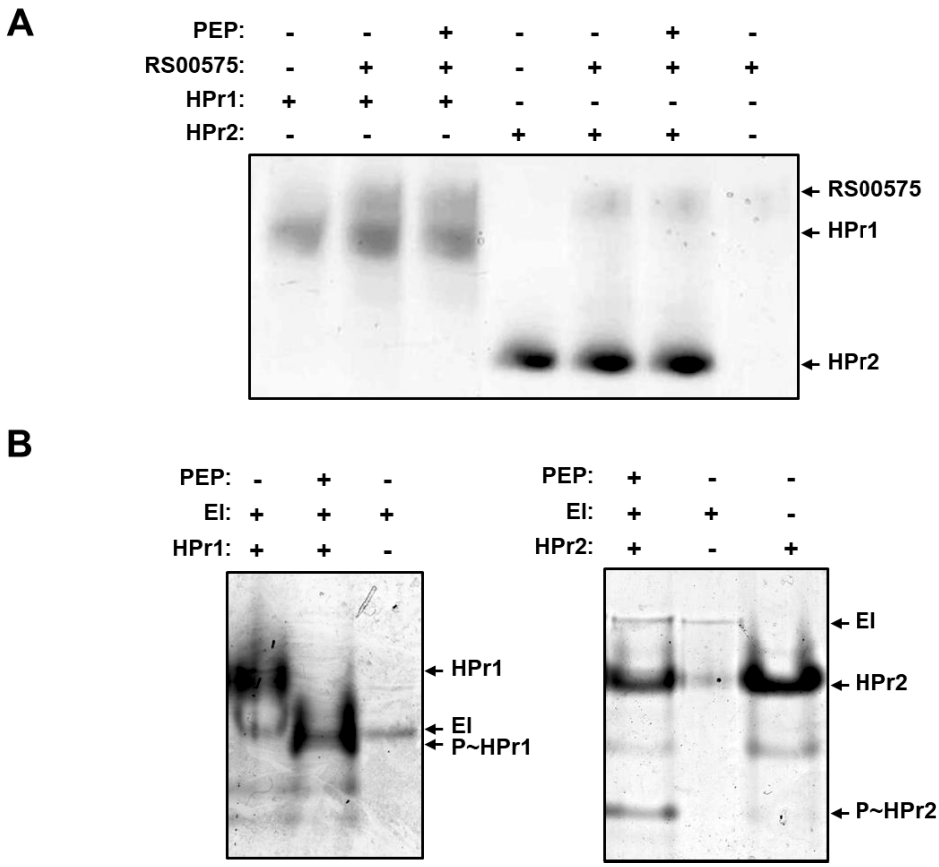

Figure 3. Identification of EI participating in PEP-dependent phosphotransfer reaction

The proteins encoded by GXM22_RS00575 (A) or GXM22_RS01250 (EI) (B) (1 μg each) were purified and incubated with either HPr1 (3 μg) or HPr2 (2 μg) in buffer P (10 mM sodium phosphate, pH 8.0; 2 mM MgCl2; 1 mM EDTA; 10 mM KCl; and 5 mM DTT) in the presence or absence of 1 mM PEP, to test the phosphotransferase activity of EI homologs. Each reaction mixture was analyzed by conducting native-PAGE to measure the electrophoretic mobility shifts of HPrs as described in the "Materials and methods" section. Panel (A) adapted from "Characterization of the PTS in the beneficial human gut bacterium *Faecalibacterium prausnitzii* A2-165," by Ham H., 2019, Dissertation, Seoul National University, p. 24.

2.2.2 Sugar-specific components of the PTS

Analysis of the *F. prausnitzii* genome sequence shows four different sugar families: glucose/maltose, NAG, fructose, and mannose (Figure 2). Since genetic manipulation is not feasible in *F. prausnitzii*, genetic mutants of sugar-specific PTS components could not be constructed. Thus, similar *in vitro* phosphotransferase assay was performed to observe the functioning of sugar-specific PTS and account for the substrate specificities of each PTS membrane proteins. In order to achieve this, HPr1 was mainly used since HPr1 could much more effectively transfer the phosphate group to EIIA (Figure 10).

3. Galactose-1-phosphate uridylyltransferase

The Leloir pathway of galactose metabolism is a highly conserved metabolism present in eukaryotic organisms such as animals and plants, and also in microbial cells. When a galactose enters the cell through its transporter, it is converted to galactose 1-phosphate (gal 1-P) by galactose kinase (GalK). Galactose-1-phosphate uridylyltransferase (GalT) then catalyzes the nucleotide exchange between uridine 5'-diphosphate glucose (UDP-glc) and gal 1-P, producing uridine 5'-diphosphate galactose (UDP-gal) and glucose 1-phosphate (glc 1-P) (Leloir, 1971). The Histidine-166 residue serves as the nucleophilic catalyst. In this cataboilic pathway, GalT plays a major role by equilibrating uridylated sugars, usually needed for the synthesis of glycosylated proteins and lipids, and extrapolymeric saccharides (Geeganage *et al*., 2000). In human, mutations in GalT is known to cause galactosemia, leading to intracellular accumulation of galactose and gal 1-P which may thus result in brain damage and neurodevelopmental problems in early ages or

learning disorders, mental retardations, and ovarian cancer later in life depending on the severity of the disease (Geeganage *et al*., 2000).

In bacteria, GalT has been extensively studied in *E. coli*, and the enzyme was reported as a dimeric protein with a molecular mass of 80 kDa consisted of two subunits, requiring metal ions for its activity (Lemaire and Mueller-Hill, 1986). When the His-166 in the active site attacks the UDP-glc, the enzyme forms a high-energy uridylyl-enzyme, displacing glc 1-P. The uridylyl-enzyme next reacts with gal 1-P, producing UDP-gal. The products of a reaction are known as competitive inhibitors of its reverse reaction. In addition, high levels of substrates were reported to be inhibitory as well (Geeganage *et al*., 2000). In *E. coli,* the absence of GalT has caused a severe growth defect, while complementation of the galT deletion strain with a galT-like gene of *Acidithiobacillus ferrooxidans* has generated rescue in growth defect (Barreto *et al.*, 2005). Thus, investigating the characteristics and regulation of GalT may be important in illustrating how bacteria may behave in the presence of galactose.

4. The aims and objectives of this study

4.1 Research Aims

The ultimate goal of this research is to present an overall framework of the PTS in *F. prausnitzii*, so that it may contribute to understanding how *F. prausnitzii* transports and metabolizes nutrients through the PTS in the intestinal environment, and how various physiological actions of bacteria are regulated accordingly upon consumption of saccharides commonly present in the human gut.

4.2 Research objectives

4.2.1 Present an overview of the PTS in *F. prausnitzii* A2-165

In the *F. prausnitzii* A2-165 genome, two homologs of EI and HPr were discovered together with HPrK, and 12 carbohydrate-specific EII proteins that form complexes for the translocation of four putative sugars: Glucose, Mannose, *N*-acetylglucosamine (NAG), and Fructose. Since genetic manipulation is not feasible in *F. prausnitzii*, *in vitro* phosphotransferase assay was performed with purified PTS proteins and membranous protein fractions extracted from *F. prausnitzii* cultured on cognate PTS sugar to reveal the expression of the functional sugar-specific PTS components. Based on these experimental data, new annotations of the functionally verified PTS components are suggested, since the previous annotations of the PTS components identified *in silico* were incorrect or turned out as non-functional (Figure 2).

4.2.2 Provide evidence to the regulatory role of the PTS component with HPr2

The genome of *F. prausnitzii* A2-165 is unique in that contrary to only two functioning sugar-specific PTS families, it possesses two copies of each of the general PTS components and that are functionally different between the two homologs, suggesting a dominant function of the PTS in regulating cell physiologies than the transportation of nutrients. Whereas HPr1 is only capable of being phosphorylated at His-15, the HPr2 in *F. prausnitzii* is also phosphorylated at Ser-46 residues by ATP-dependent mechanism as in *B. subtilis.* Therefore, pieces of evidence suggesting the regulatory function of HPr2 in cellular pathways other than

PTS are investigated.

Next, to find the binding partners of HPr2, the ligand-bait fishing technique is performed using the cell lysate of *F. prausnitzii* A2-165 grown on a glucose medium, in which various phosphorylation forms of HPr2 is expected to be present. The binding partner, identified as galactose-1-phosphate uridylyltransferase (GalT) in *F. prausnitzii*, is purified and tested for binding specificity with HPr2. The activity of GalT is studied through coupled enzyme assay.

II. Materials and Methods

1. Strains and plasmids

Genomic DNA of *F. prausnitzii* A2-165 (DSMZ) was used as the template DNA for cloning. *E. coli* ER2566△pts (NEB; Nosworthy *et al*, 1998), carrying a chromosomal copy of the T7 RNA polymerase gene under the control of the lac promoter (Steen *et al*., 1986) as well as the deletion of the *pts* genes, was used for the overproduction of recombinant proteins. The expression vector pETDuet-1 (Novagen), which contain an ampicillin resistance gene and a T7 promoter/*lac* operator, was used to construct the overexpression vectors of His-tagged and untagged proteins.

2. Media and cell culture

Yeast extract-casein hydrolysate-fatty acids (YCFA) medium was used for the culture of *F. prausnitzii* (Duncan *et al*., 2003). The medium contained (per 200 ml): 2 g of Casitone, 0.5 g of yeast extract, 1 g of glucose, 9 mg of $MgSO_4 \cdot 7H_2O$, 18 mg of $CaCl_2 \cdot 2H_2O$, 90 mg of K_2HPO_4 and KH_2PO_4, 0.18 g of NaCl, 0.2 mg of resazurin, 0.8 g of $NaHCO_3$, 0.2 g of L-Cysteine-HCl, 2 mg of hemin, supplemented with a filter-sterilized vitamin solution consisting of 2 μg of biotin and folic acid, 10 μg of pyridoxine-HCl, 5 μg of thiamine-HCl$\cdot 2H_2O$, D-Ca-pantothenate, riboflavin, and nicotinic acid, 0.1 μg of vitamin B_{12}, and 5 μg of p-Aminobenzoic acid, and lipoic acid. Short-chain fatty acids (SCFA) were added to make final concentrations

(vol/vol) of 0.19% acetic acid, 0.07% propionic acid, 0.009% isobutyric acid, 0.01% *n*-valeric and isovaleric acid.

Luria Bertani (LB) broth consisting of 1% tryptone, 0.5% NaCl and 0.5% yeast extract was used for routine bacterial culture. The antibiotics ampicillin (100 μg/ml), kanamycin (20 μg/ml), and ciprofloxacin (1 μg/ml) were added when required.

3. Recombinant DNA techniques

3.1 Preparation of genomic DNA

Genomic DNA (gDNA) from *F. prausnitzii* A2-165 was extracted using the QIAamp DNA Mini Kit according to the manufacturer's instructions (QIAGEN). The eluted DNA was aliquoted in 1.5 ml microcentrifuge tubes to a final concentration of 350 ng/μl.

3.2 Construction of recombinant plasmids

The PTS genes were identified using NCBI and KEGG databases and recombinant plasmids were constructed with either no tags or hexahistidine tags using pETDuet-1 vector. The strains and recombinant plasmids used in this study are listed in Table 2.

3.3 Site-directed mutagenesis

The Serine-110 residue of the EIIA domain of $EIIABC^{Fru}$ was substituted to aspartate (S110D), and the Ser-10 and Ala-16 of EIIA (GXM22_RS04190) were substituted with Asp (RS04190 [SA→D]) to observe the phosphorylation-dependent electrophoretic mobility shift. To observe the phosphorylation-dependent binding of

HPr2 with GalT, the Histidine-15 and Serine-46 residues were substituted to alanine (H15A or S46A) and or aspartate (H15D and S46D) to mimic the dephosphorylated and phosphorylated state of HPr2, respectively.

4. Protein expression and purification

4.1 Overexpression of proteins

E. coli ER2566△*pts* transformed with strains indicated in Table 1 was used for the overexpression of both cytoplasmic and membrane PTS proteins. Cells were grown in LB medium at 37°C until the culture reached A_{600} of 0.5, at which 1 mM of IPTG (isopropyl β-D-1-thiogalactopyranoside) was added to the culture medium. After 3-4 hours of induction, the cells were harvested at 9,300 x *g* for 5 minutes.

4.2 Purification of proteins

Proteins were expressed from pETDuet-1 vectors in *E. coli* ER2566 △*pts* (Park *et al.*, 2013) (Table 2). Harvested cells were resuspended in buffer A (20 mM sodium phosphate, pH 8.0; 5 mM β-mercaptoethanol; and 5% glycerol) containing 200 mM NaCl and then disrupted by ultrasonication. The cell lysates were centrifuged at 100,000 × *g* at 4°C for 1 h to remove cell debris. Untagged proteins were purified using the MonoQ™ 10/100 GL and the HiLoad 16/60 Superdex 200 prep grade columns (GE Healthcare Life Science, Marlborough, MA). After removal of cell debris, the lysate was applied to a Mono Q™ 10/100 GL (GE Healthcare Life Science) column equilibrated with buffer A, containing 50 mM NaCl. The protein fraction was eluted using buffer A with 0.05 to 1 M NaCl gradient at a flow rate of 2 mL min^{-1}. The fractions containing the desired proteins were concentrated using

Amicon Ultracel-3K centrifugal filters (Merck Millipore, Burlington, MA) and were subjected to chromatography using the HiLoad 16/60 Superdex 200 prep grade column (GE Healthcare Life Science) equilibrated with buffer A containing 200 mM NaCl (buffer B) to achieve higher purity.

His-tagged proteins were purified by performing immobilized metal affinity chromatography using a TALON metal affinity resin (Takara Bio Inc., Otsu, Japan) according to the manufacturer's instructions. Resin-bound proteins were subjected to washing steps three times using buffer B containing 10 mM imidazole and eluted with 200 mM imidazole. To remove imidazole and increase purity, proteins were subjected to chromatography using the HiLoad 16/600 Superdex 200 prep grade column (GE Healthcare Life Science) equilibrated with buffer B. His-tagged $EIICB^{NAG}$ was purified from the *E. coli* cell membrane after solubilization with 1% n-dodecyl-β-D-maltopyranoside (DDM). After removal of cell debris from the lysate, the membrane was centrifuged at 100,000 × *g* at 4°C for 1 h to obtain the membrane in a pellet form. The pellet was resuspended in buffer B containing 1% DDM and centrifuged again at 100,000 × *g* at 4°C for 30 min. His-$EIICB^{NAG}$ was purified using a TALON metal affinity resin (Takara Bio Inc.) as described above, except for the addition of 0.1% DDM in wash and elution buffer. The eluted proteins were further chromatographed on the HiLoad 16/600 Superdex 200 prep grade column (GE Healthcare Life Science) equilibrated with buffer B containing 0.05% DDM. Purified proteins were concentrated using Amicon Ultracel-3K centrifugal filters (Merck Millipore), and total protein concentration was determined by performing the Bradford protein assay using bovine serum albumin as the standard.

4.4 Extraction of the membrane proteins from *F. prausnitzii*

F. prausnitzii A2-165 cells grown on the indicated sugars were harvested after 36 h, subjected to washing steps with buffer C (20 mM Tris-HCl, pH 8; 150 mM NaCl; 1 mM phenylmethylsulfonyl fluoride; 10 mM $MgCl_2$; 10% glycerol; and 5 mM β-mercaptoethanol) and centrifuged at 9,300 × *g* at 4°C for 15 min. The cell pellet obtained after centrifugation was resuspended in buffer C and frozen at -80°C with the addition of protease inhibitor (Sigma-Aldrich, Waltham, MA) to lyse the cells. The cells were disrupted by ultrasonication and then centrifuged at 9,300 × *g* at 4°C for 15 min to remove cell debris. The cell lysates were further centrifuged at 100,000 × *g* at 4°C for 1 h, and the resulting pellets were resuspended in buffer B containing 1% DDM. The solubilized membrane fraction was centrifuged at 10,000 × *g* at 4°C for 20 min to remove any remaining debris.

5. *In vitro* phosphorylation assay

All phosphorylation assays were performed using buffer P (10 mM sodium phosphate, pH 8.0; 2 mM $MgCl_2$; 1 mM EDTA; 10 mM KCl; and 5 mM DTT) and the following purified proteins, if not indicated otherwise: 1 μg of EI homologs, 3 μg of HPr1, 2 μg of HPr2, 1 μg of HPrK/P, and 1 μg of EIIAs. The reaction mixtures, if not indicated otherwise, were incubated for 10 min at 37°C in the presence of 1 mM PEP, 1 mM pyruvate, or 4 mM ATP. Each reaction mixture was subjected to analysis on a 4 to 20% gradient or 16% polyacrylamide gel for SDS-PAGE and 10% for native-PAGE (acrylamide/bisacrylamide ratio of 37.5:1) (KOMA Biotech Inc., Seoul, South Korea) in Tris-Glycine (25 mM Tris, 192 mM Glycine) buffer supplemented with or without 0.1% SDS followed by Coomassie Brilliant Blue R staining. PTS-dependent sugar phosphorylation assays were conducted in an

identical manner using three soluble PTS proteins (1 μg of EI, 3 μg of HPr1, and 2 μg of EIIAs), 0.5 μg of $EIICB^{NAG}$, and 4 μg of total membrane protein extracts in combinations as indicated. The reaction mixtures were incubated for 10 min at 37°C in the presence of 0.1 mM PEP and 2 mM of the indicated carbohydrates. The protein band intensities were quantified using the ImageJ software (NIH Image, National Institutes of Health, Bethesda, MD; available online at http://rsbweb.nih.gov/ij/).

6. RNA extraction and reverse transcription-PCR (RT-PCR)

F. prausnitzii A2-165 cells cultured overnight were diluted 100-fold in 10 mL of fresh YCFA medium supplemented with the indicated filter-sterilized carbon sources in 0.5% (w/v) final concentration and incubated at 37°C until OD_{600} reached 0.4 for galactose and glucose and 0.2 for fructose and NAG. After fixing the cells with the same volume of 100% methanol for 1 h at -20°C, total RNA was extracted using the phenol-chloroform extraction method (Kim *et al.*, 2020); the isolated RNAs were further purified using the TaKaRa MiniBEST Universal RNA Extraction Kit (Takara Bio Inc.) according to the manufacturer's instructions. Two biological replicates were performed for each sample.

To conduct RT-PCR analysis, total RNA from each sample (2,500 ng) was converted to cDNA using the RNA to cDNA EcoDry Premix Random Hexamers (Clontech Laboratories Inc., Mountain View, CA). RNA, genomic DNA, and cDNA were used as templates to verify the presence of the transcription units of *ptsI* (GXM22_RS01250) and *ptsH* (GXM22_RS01245) using the appropriate primers (Park *et al.*, 2016).

7. Ligand fishing and protein-protein interaction test using metal affinity chromatography

F. prausnitzii cells grown for 36 hours in YCFA-glucose medium were harvested and subjected to washing steps with buffer C and centrifuged at 9,300 × *g* at 4°C for 15 min. The cell pellet obtained after centrifugation was resuspended in buffer C and frozen at -80°C with the addition of protease inhibitor (Sigma-Aldrich, Waltham, MA) to lyse the cells. The cells were disrupted by ultrasonication and then centrifuged at 9,300 × *g* at 4°C for 15 min to remove cell debris. The cell lysates were further centrifuged at 100,000 × *g* at 4°C for 1 h, and the supernatant containing cytosolic proteins was divided into aliquots and mixed either with a His-tagged protein as a bait or with binding buffer as a control. Each mixture was then incubated with 50 ul TALON metal affinity resin in a 1.5 ml tube at 4°C for 20 min. After two brief washes with the binding buffer containing 10 mM imidazole, proteins bound to the resin were eluted with the binding buffer containing 200 mM imidazole. Aliquots of the eluted protein sample were analyzed by 4 to 20% SDS-PAGE and stained with Coomassie brilliant blue. Protein bands specifically bound to the His-tagged bait protein were excised from the gel, and in-gel digestion and peptide mapping of the tryptic digests were performed as described previously using MALDI-TOF MS (Park *et al*., 2013).

The interaction test between the purified GalT and HPr2 phosphomimetic mutants, or between GalT overexpression lysate and wild-type HPr2 were performed in an identical process.

8. Size exclusion chromatography (SEC)

GalT was expressed and purified from *E. coli*, and then was analyzed by size exclusion chromatography to measure the molecular size of the enzyme. Standard curve of size exclusion chromatography was generated with size marker proteins: Blue dextran (2,000 kDa), Thyroglobulin (669 kDa), Apoferritin (443 kDa), β–amylase (200 kDa), Alcohol dehydrogenase (150 kDa), Albumin (66 kDa), and Carbonic anhydrase (29 kDa). The superdex 200 column was equilibrated with 50 mM Tris-HCl (pH 7.5), 100 mM KCl, 10% glycerol, 200 mM NaCl, and 10 mM DTT according to the manufacturer's protocol.

9. Enzyme assay

To observe the activity of GalT, the reaction was measured by coupling the production of glc 1-P to the reduction of $NADP^+$ in the presence of phosphoglucomutase (PGM) and glucose 6-P dehydrogenase (G6PDH). All enzyme assays were performed using buffer E (20 mM Sodium phosphate pH 8.0, 5 mM DTT, 2.5 mM MgCl2, 8 mM Cystein-HCl, 10 μg/ml BSA) and the following purified proteins if not indicated otherwise: 5 μg of GalT, 18.6 μg of PGM, and 5 μg of G6PDH. The reaction mixtures, if not indicated otherwise, were incubated for 5 min at 37°C in the presence of 0.2 mM $NADP^+$, 1 mM UDP-Glc, and the reaction was started by adding 1 mM Gal 1-P to the reaction mixture, in a final volume of 1 ml. The formation of NADPH was measured spectrophotometrically (Shimadzu UV-1240, Seoul, South Korea) at 340 nm for 5 min.

Table 2. Bacterial strains and plasmids used in this study

Strains or plasmids	Genotypes and/or descriptions	References or source
Strains		
Escherichia coli		
ER2566	F⁻ λ⁻ *fhuA2* [*lon*] *ompT lacZ*::T7 gene 1 *gal sulA*11 △(*mcrC-mrr*)114::IS10 R(*mcr*-73::miniTn10-TetS)2 R(*zgb*-210::Tn10) (TetS) *endA1* [*dcm*]	New England Biolabs
ER2566△*pts*	ER2566 *ptsHIcrr*::Km^r	(Park *et al.*, 2013)
Rosetta/pLysSRARE	F-ompT hsdSB(rB- mB-) gal dcm (DE3) pLysSRARE (CamR)	Sigma-Aldrich
Faecalibacterium prausnitzii		
A2-165 (DSM 17677)		DSMZ
Plasmids		
pETDuet-1		Novagen
pETDuet_EI	pETDuet-1-based expression vector for EI, Apr	This study
pETDuet_RS00575	pETDuet-1-based expression vector for RS00575, Apr	This study
pETDuet_HPr1	pETDuet-1-based expression vector for HPr1, Apr	This study
pETDuet_HisHPr1	pETDuet-1-based expression vector for His_6 tagged-HPr1, Ap^r	This study
pETDuet_HPr2	pETDuet-1-based expression vector for HPr2, Apr	This study
pETDuet_HisHPr2	pETDuet-1-based expression vector for His_6 tagged-HPr2, Ap^r	This study
pETDuet_HisHPr2 (H15A)	pETDuet-1-based expression vector for His_6 tagged-HPr2 (H15A), Ap^r	This study
pETDuet_HisHPr2 (H15D)	pETDuet-1-based expression vector for His_6 tagged-HPr2 (H15D), Ap^r	This study
pETDuet_HisHPr2 (S46D)	pETDuet-1-based expression vector for His_6 tagged-HPr2 (S46D), Ap^r	This study
pETDuet_HisHPr2 (H15A, S46D)	pETDuet-1-based expression vector for His_6 tagged-HPr2 (H15A, S46D), Ap^r	This study
pETDuet_HisHPr2 (H15D, S46D)	pETDuet-1-based expression vector for His_6 tagged-HPr2 (H15D, S46D), Ap^r	This study
pETDuet_HisEIIA^{NAG}	pETDuet-1-based expression vector for His_6 tagged-EIIA^{NAG}, Ap^r	This study

pETDuet_HisEIIA^{Fru}	pETDuet-1-based expression vector for His_6 tagged-EIIA domain (S110D) of FruA, Ap^r	This study
pETDuet_EIIA^{04190}	pETDuet-1-based expression vector for EIIA^{04745}, Ap^r	This study
pETDuet_HisEIIA^{04190} (S10D A16D)	pETDuet-1-based expression vector for His_6 tagged EIIA^{04745} (S10D A16D), Ap^r	This study
pETDuet_EIIA^{01370}	pETDuet-1-based expression vector for EIIA01370, Apr	This study
pETDuet_HisHprK/P	pETDuet-1-based expression vector for His_6 tagged-HPrK/P, Ap^r	This study
pETDuet_HisGalT	pETDuet-1-based expression vector for His_6 tagged-GalT, Ap^r	This study
pET24a		Novagen
pET24a_GalT	pET24a-based expression vector for FpGalT, Km^r	This study
pET28a		Novagen
pET28a_EcG6PDH	pET24a-based expression vector for His_6 tagged-EcG6PDH, Km^r	This study
pET28a_EcPGM	pET24a-based expression vector for His_6 tagged-EcPGM, Km^r	This study

[a]Km^r, kanamycin-resistant; Ap^r, ampicillin-resistant; CamR: chloramphenicol-resistant

III. Results

1. Functional studies on sugar-specific PTS proteins of *F. prausnitzii* A2-165

1.1 *F. prausnitzii* A2-165 has functional *N*-acetylglucosamine-PTS

To observe the phosphorylation of PTS sugars by the cognate PTS proteins in *F. prausnitzii*, and to identify the sugar specificities of the PTS membrane components, membrane proteins were extracted from *F. prausnitzii* cells grown on a single carbohydrate as the sole carbon source. Then an *in vitro* phosphotransferase assay was performed by mixing the membrane protein extracts with purified EI, HPr1, and EIIA in the presence of PEP and various carbohydrates. I assumed that, if the PTS-membrane proteins are expressed in cells grown on a PTS carbohydrate, the cognate EIIA will be dephosphorylated upon the addition of that sugar, since the phosphate group will be transferred from EIIA to the EII complex in the membrane, and finally to the incoming PTS sugar molecule. Therefore, the phosphorylation state of EIIA would represent the presence of functional carbohydrate-specific PTS proteins in the membrane protein extract (Figure 4).

Since glucose was consumed by all *F. prausnitzii* strains (Duncan *et al.*, 2002; Lopez-Siles *et al.*, 2012), I anticipated that the glucose/glucoside-specific EIIA should be dephosphorylated in the presence of glucose and the membrane proteins extracted from glucose-grown *F. prausnitzii* cells. However, EIIA

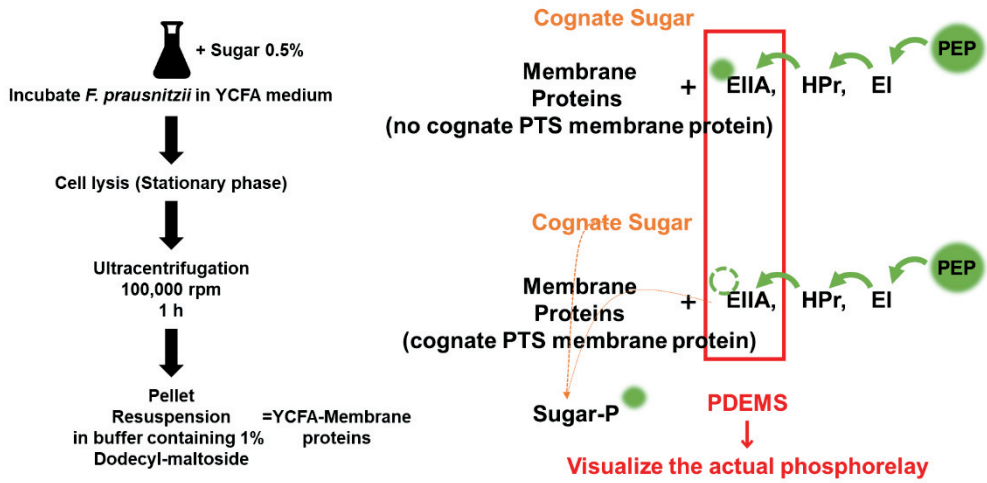

Figure 4. Functional studies on sugar-specific PTS proteins

To observe the phosphorylation of PTS sugars by the cognate PTS proteins in *F. prausnitzii*, and to identify the sugar specificities of the PTS membrane components, membrane proteins were extracted from *F. prausnitzii* cells grown on a single carbohydrate as the sole carbon source. Then an *in vitro* phosphotransferase assay was performed by mixing the membrane protein extracts with purified EI, HPr1, and EIIA in the presence of PEP and various carbohydrates. The phosphorylation state of EIIA would represent the presence of functional carbohydrate-specific PTS proteins in the membrane protein extract. PDEMS; phosphorylation-dependent electrophoretic mobility shift.

(GXM22_RS01420) was not dephosphorylated when glucose was added to the mixture of the membrane proteins extracted from glucose-grown cells in the presence of PEP, EI, and HPr1 (Figure 5A). Interestingly, however, EIIA was dephosphorylated only when NAG was added to the mixture containing membrane proteins extracted from NAG-grown cells (Figure 5A). Based on this result, I annotated the EIIA encoded by GXM22_RS01420 as an EIIA specific for NAG ($EIIA^{NAG}$). To determine whether the functional NAG-specific PTS membrane protein was $EIICB^{NAG}$ encoded by GXM22_RS00590, annotated as *nagE* (Figure 2 and Table 1), the putative $EIICB^{NAG}$ was overexpressed and purified in *E. coli*. Purified $EIICB^{NAG}$ was then mixed with EI, HPr1, and $EIIA^{NAG}$ in the presence of PEP and a carbohydrate such as glucose, NAG, fructose, mannose, or glycerol. As a result, $EIIA^{NAG}$ was dephosphorylated completely upon the addition of NAG and to some extent (~20%) upon the addition of glucose (Figure 5B, lanes Glc and NAG). Thus, $EIICB^{NAG}$ seemed to have NAG as its main substrate and glucose with a much lower affinity. The results, therefore, show that $EIICB^{NAG}$ is expressed as a functional protein from *nagE* in *F. prausnitzii* A2-165 when the bacterium is consuming NAG.

1.2 *F. prausnitzii* A2-165 has functional fructose-PTS

Next, the import of fructose through the PTS was examined because fructose could also be efficiently utilized by all *F. prausnitzii* strains tested (Duncan *et al.*, 2002; Lopez-Siles *et al.*, 2012). The putative fructose-specific EIIABC is encoded by *fruA* (GXM22_RS09805) in *F. prausnitzii* A2-165 (Table 1). To confirm whether the fructose PTS components were specifically expressed in response to fructose as

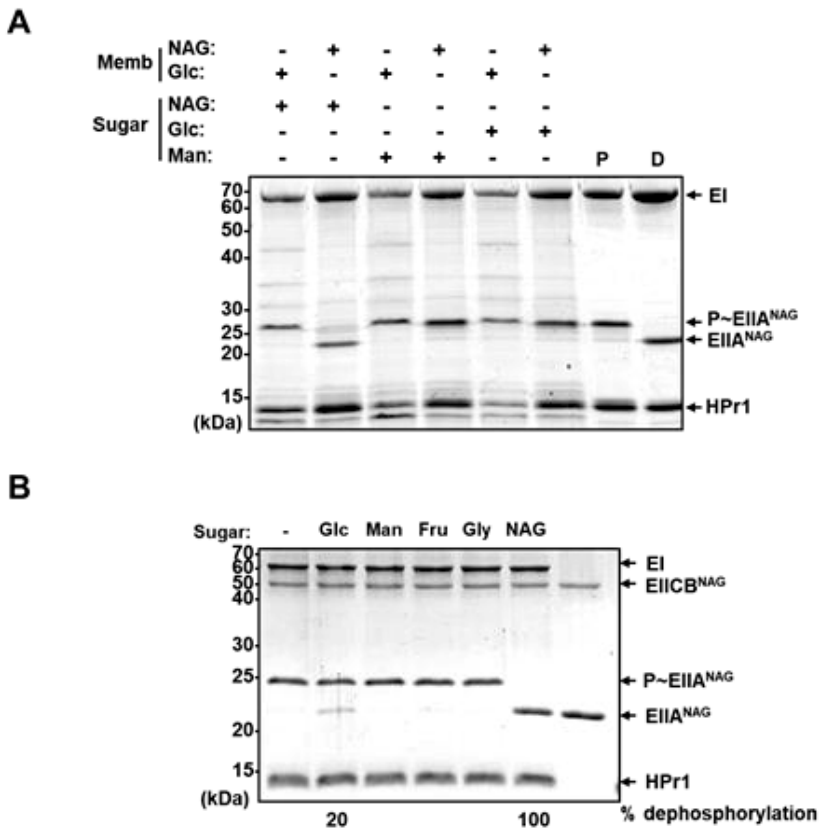

Figure 5. Detection of the sugar phosphorylation activity of *N*-acetylglucosamine-specific enzyme II

In vitro phosphotransferase assays were performed to measure the sugar phosphorylation activity of the membrane protein extracts (A) and purified $EIICB^{NAG}$ (B). Membrane protein extracts (Memb) were prepared from *F. prausnitzii* cells grown on glucose or NAG as indicated. The membrane protein extract (4 μg) or purified $EIICB^{NAG}$ (0.5 μg) was incubated with three soluble PTS proteins (1 μg of EI, 3 μg of HPr1, and 1 μg of $EIIA^{NAG}$) in buffer P in the presence of 0.1 mM PEP and the indicated recipient sugars (2 mM). Reaction mixtures with EI, HPr1, $EIIA^{NAG}$ in the presence (lane P) or absence (lane D) of 0.1 mM PEP without the addition of any membrane fractions and recipient sugars served as a control. NAG, *N*-acetylglucosamine; Man, mannose; Fru, fructose; Gly, glycerol. Panel (B) adapted from "Characterization of the PTS in the beneficial human gut bacterium *Faecalibacterium prausnitzii* A2-165," by Ham H., 2019, Dissertation, Seoul National University, p. 28.

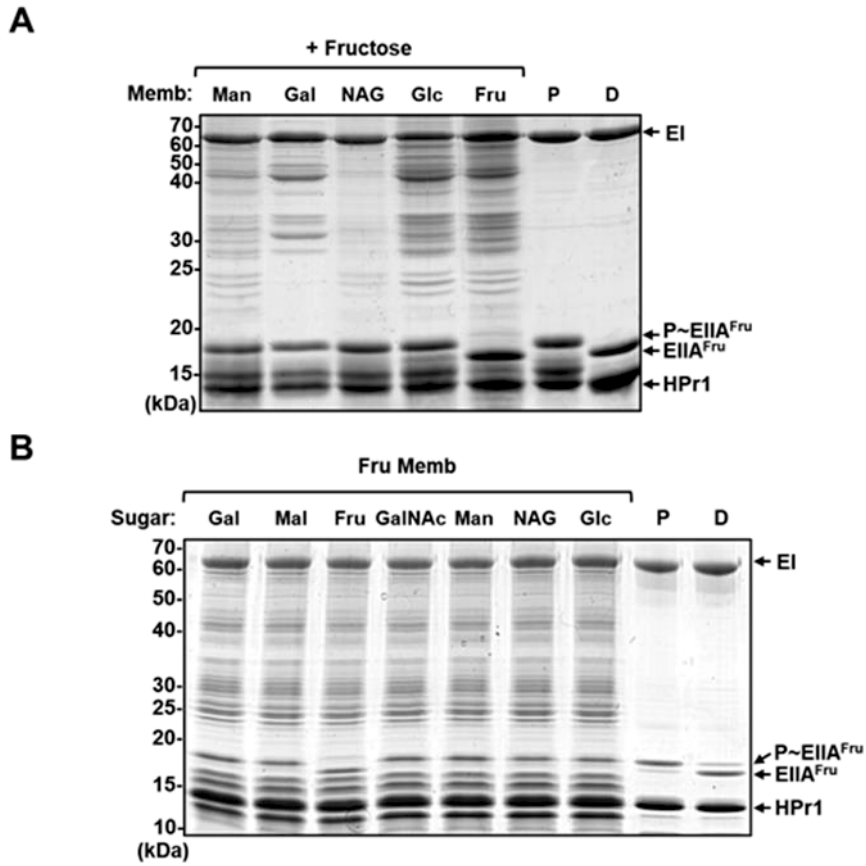

Figure 6. Fructose-specific enzyme II is expressed exclusively in the presence of fructose

In vitro phosphotransferase assays were performed to investigate the expression condition and substrate specificity of EIIABC^{Fru}. (A) Membrane protein extracts (Memb) were prepared from *F. prausnitzii* cells grown on the indicated sugars and each extract (4 μg) was incubated with EI (2 μg), HPr1 (3 μg), and EIIA^{Fru}(S110D) (2 μg) in buffer P in the presence of 0.1 mM PEP and 2 mM of fructose. (B) The membrane protein extract prepared from *F. prausnitzii* cells grown on fructose was incubated with EI (2 μg), HPr1 (2 μg), and EIIA^{Fru}(S110D) (1 μg) in buffer P in the presence of 0.1 mM PEP and 2 mM of the indicated sugar. Reaction mixtures were analyzed by conducting SDS-PAGE to measure the electrophoretic mobility shifts of EIIA^{Fru}. The reaction mixture in the presence (lane P) or absence (lane D) of 0.1 mM PEP without the addition of any membrane fractions or sugars served as a control. Gal, galactose; Mal, maltose; GalNAc, *N*-acetylgalactosamine.

shown in Figure 1, EI, HPr1, EIIA^{Fru}(S110D), and PEP were mixed with fructose and the membrane proteins extracted from cells grown on various carbohydrates including mannose, galactose, NAG, glucose, and fructose. This result showed that EIIA^{Fru}(S110D) could be dephosphorylated by fructose only when the membrane proteins extracted from the cells grown on fructose were added (Figure 6A). Next, to observe the sugar specificity of FruA, the membrane protein extract of fructose-grown cells was mixed with the general PTS components, EIIA^{Fru}(S110D), PEP, and various carbohydrates. As a result, EIIA^{Fru}(S110D) could be dephosphorylated only in the presence of fructose but not in the presence of galactose, maltose, NAG, glucose, mannose, and *N*-acetylgalactosamine (GalNAc) (Figure 6B). Therefore, I conclude that FruA is expressed specifically in the presence of fructose, and the fructose-PTS only participates in the transportation of fructose in *F. prausnitzii* A2-165.

1.3 Non-functional or cryptic PTS components

It has been previously reported that *F. prausnitzii* A2-165 could not metabolize mannose: the mannose-catabolism gene cluster exists only in some strains of *F. prausnitzii*, other than A2-165 (Martín *et al.*, 2017; Fitzgerald *et al.*, 2018). I, therefore, tested their functionality by conducting *in vitro* phosphotransferase assay to observe the PDEMS in native- or SDS-PAGE in the presence of PEP, as shown in Figure 4. Interestingly, GXM22_RS04190 and GXM22_RS01370 encoding EIIAs have highly similar sequences (72%) (Figure 7A). The two mannose-family EIIAs did not demonstrate any PDEMS on native-PAGE gels in the presence of PEP and general PTS components (Figure 7B and 7E). In addition, when the identical

sets of samples were subjected to analysis by SDS-PAGE, I could not observe a phosphorylation-dependent upshift of the two putative mannose-specific EIIAs (Figure 7C and 7F). Hence, in a final effort to visualize phosphorylation at His-9, if it ever occurs, I substituted Ser-10 and Ala-16 of EIIA (GXM22_RS04190) with aspartate (SA→D) to induce PDEMS in SDS-PAGE (Lee *et al.*, 2019). Despite the introduction of negative charges nearby the expected phosphorylation site of His-9 (Figure 7A), the EIIA encoded by GXM22_RS04190 did not demonstrate PDEMS in the presence of PEP, whereas $EIIA^{NAG}$ did (Figure 7D, lanes 2 and 4). Hence, I conclude that both GXM22_RS04190 and GXM22_RS01370 are non-functional and so are the contiguous EIIBC or D (GXM22_RS04185 to RS04175 and GXM22_RS01340 to RS01350).

Since I have confirmed that the membrane proteins extracted from cells grown on a PTS sugar contain the cognate PTS components, as seen in fructose- or NAG-grown cells (Figure 5A and 6A), I assumed that the EIIBC encoded by GXM22_RS14870 would be present in the membrane fraction extracted from glucose- or maltose-grown cells. To verify this assumption, I mixed purified EI, HPr1, and $EIIA^{NAG}$, which is the only functional form of the three separately encoded EIIAs, with membrane proteins extracted from glucose- or maltose-grown cells in addition to PEP, to observe whether any dephosphorylation of $EIIA^{NAG}$ occurs by the addition of glucose or maltose (Figure 8). Unexpectedly, however, I could not see any dephosphorylation of $EIIA^{NAG}$ in either of the two membrane protein extracts in the presence of glucose, maltose, GalNAc, NAG, or mannose (Figure 8A and 8B). Furthermore, EIIBC (GXM22_RS14870) did not have any activity towards other glucose-containing disaccharides (Figure 8C). Finally, since *F. prausnitzii* is known to consume glucosamine (GlcN) (Duncan *et al.*, 2002;

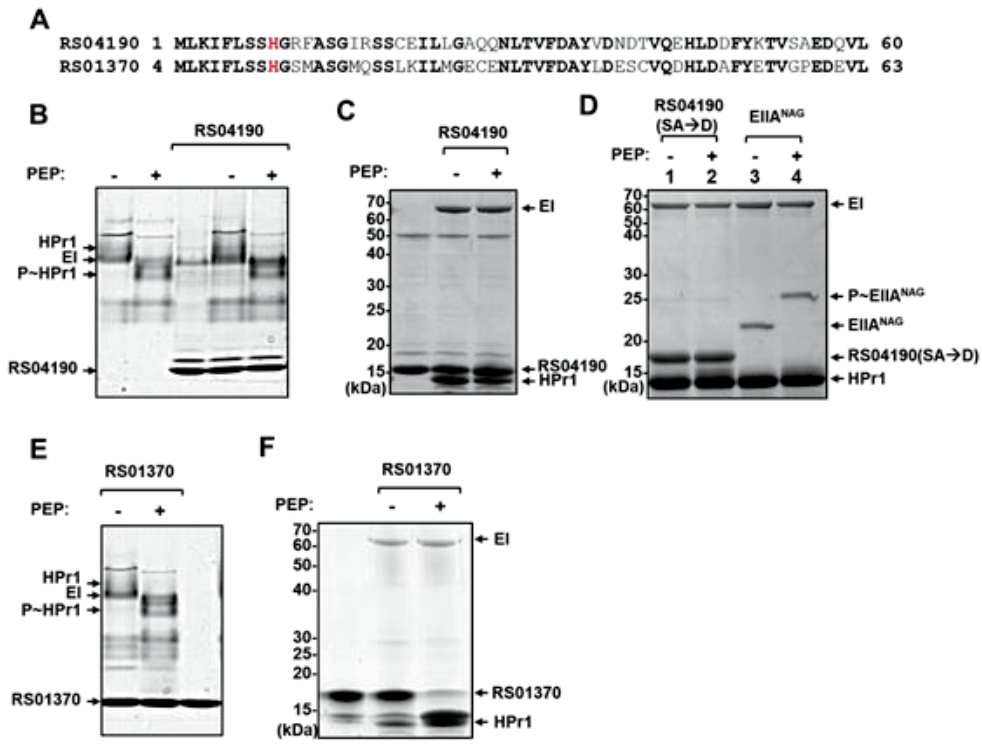

Figure 7. Putative mannose-PTS proteins are non-functional

(A) Amino acid sequence alignment of the two mannose-family EIIAs encoded by GXM22_RS01370 and RS04190. Identical amino acids are indicated in bold and the expected phosphorylation sites are indicated in red. To test the phosphotransferase activity of putative mannose-specific EIIAs, 2 μg of EIIA (GXM22_RS04190) (B and C) or EIIA (GXM22_RS01370) (E and F) was incubated with 1 μg of EI and 1 μg of HPr1 in buffer P in the presence of 0.1 mM PEP. Each reaction mixture was subjected to analysis by native-PAGE (B and E) and by SDS-PAGE (C and F) to visualize phosphorylation by PDEMS. (D) For further verification, a mutant form of EIIA (GXM22_RS04190) with Ser-10 and Ala-16 substituted with Asp (RS04190 [SA→D]) was mixed with 1 μg of EI and 3 μg of HPr1 in the presence of 0.1 mM PEP and analyzed by conducting SDS-PAGE to observe a possible PDEMS. $EIIA^{NAG}$ was included as a positive control for the phosphotransfer reaction.

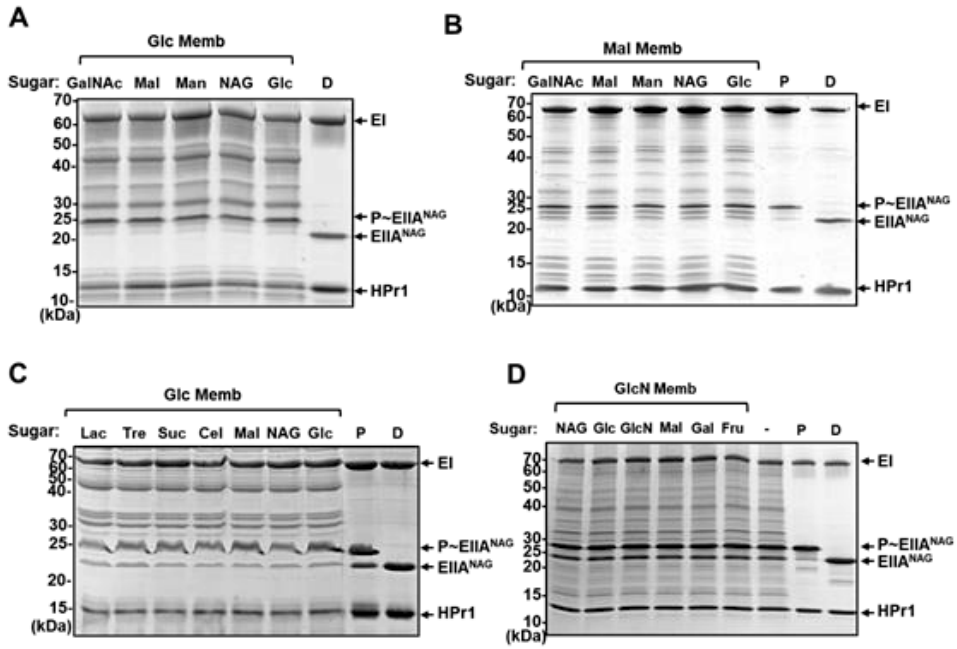

Figure 8. EIICB component encoded by GXM22_RS14870 is cryptic

To assess the functionality of the putative glucose/maltose-family EIICB (GXM22_RS14870), 4 μg of membrane protein extracts (Memb) prepared from *F. prausnitzii* cells grown on glucose **(A and C)**, maltose **(B)**, or glucosamine **(D)** were incubated with EI (1 μg), HPr1 (2 μg), and $EIIA^{NAG}$ (2 μg) in buffer P in the presence of 0.1 mM PEP and 2 mM of the indicated sugars, and subjected to SDS-PAGE. The reaction mixtures of EI, HPr1, and $EIIA^{NAG}$ in the absence (lane D) or presence (lane P) of 0.1 mM PEP without the addition of any membrane protein extract and sugar served as a control. Lac, lactose; Tre, trehalose; Suc, sucrose; Cel, cellobiose; GlcN, glucosamine.

Lopez-Siles *et al.*, 2012; Miquel *et al.*, 2014), I tried to test the possibility of GXM22_RS14870 being the PTS transporter for GlcN. Membrane protein extracts were prepared from the cells grown on GlcN and an identical phosphotransferase assay was performed (Figure 8D). As a result, I could not observe the dephosphorylation of $EIIA^{NAG}$ by the addition of GlcN to the extent greater than the addition of any other sugars or no sugar. Therefore, I conclude that EIIBC (GXM22_RS14870) is a cryptic PTS protein.

2. HPr2 may function as a regulatory protein

2.1 HPr2 is capable of being phosphorylated at Serine-46, Histidine-15, and both

It has been proposed that PTS lacking EII components as opposed to well-conserved general components may carry out regulatory functions by interacting with its target proteins than the transporting role (Deutscher et al., 2014). Hence, I tried to investigate the regulatory role of HPr2 since it is capable of being phosphorylated on its Ser-46 residue (Singh et al., 2008), taking various phosphorylated forms (Figure 9B). Whereas Hpr1 was incapable of being phosphorylated by HPrK (Figure 9A), the HPr2 could be phosphorylated also at Ser-46 residues by an ATP-dependent mechanism. The Ser-46 phosphorylation of HPr in Gram-positive bacteria has been known to be involved in numerous physiological regulations, such as amino acid metabolism and carbon catabolite repression, as a cofactor for CcpA (Stülke and Hillen, 1998) (Figure 1). The HPr2 also displayed a double phosphorylation pattern when both HPrK and EI were present with PEP and ATP. A previous study on the glycerol kinase of

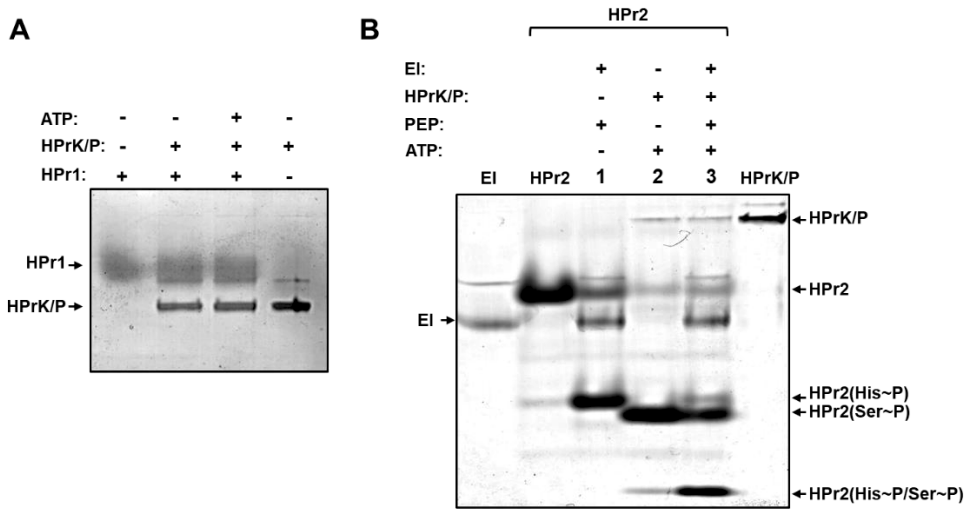

Figure 9. HPr2 can be phosphorylated by both EI and HPrK/P

(A) To test the phosphorylation of HPr1 by HPrK/P, HPr1 (3 μg) was incubated with HPrK/P (1 μg) in buffer P in the presence or absence of 4 mM ATP. (B) To test the phosphorylation of HPr2 by HPrK/P and EI, HPr2 (20 μg) was incubated with either HPrK/P or EI (3 μg each), or both (lane 1, 2, and 3, respectively), in buffer P in the presence or absence of 4 mM ATP and 4 mM PEP. Each reaction mixture was analyzed by performing native-PAGE to measure the electrophoretic mobility shifts of HPrs as described in the “Materials and methods” section.

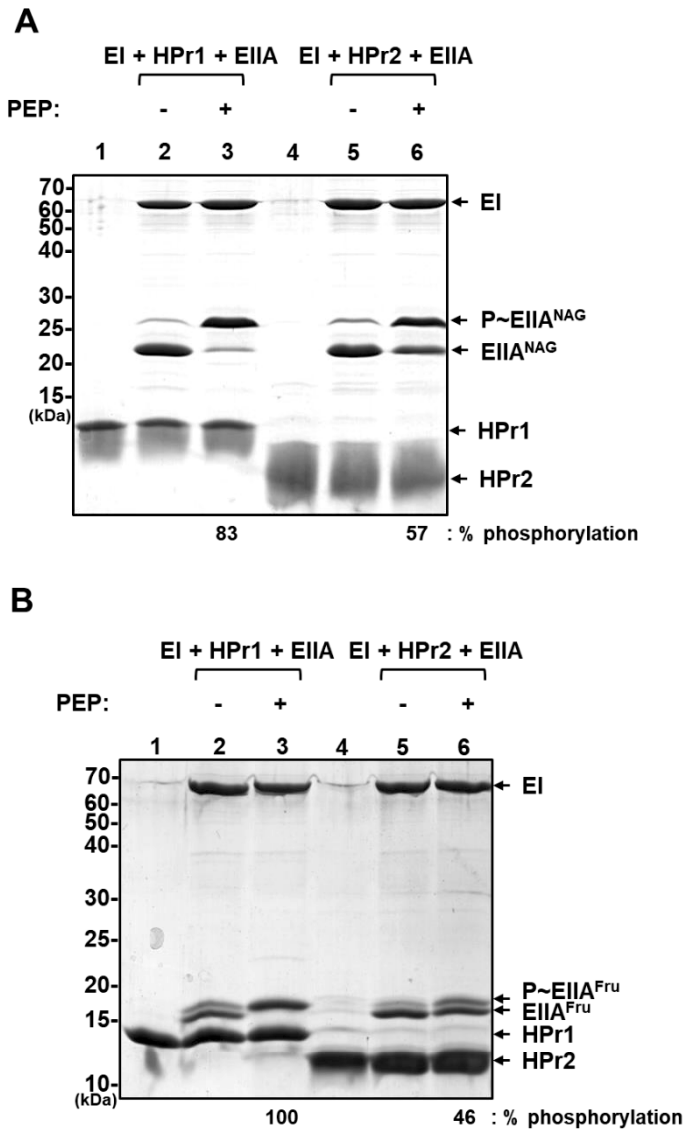

Figure 10. HPr1 is the main phosphocarrier protein mediating the PEP-dependent phosphotransfer reaction

To test the phosphotransferase activity of HPrs, either HPr1 (lanes 1 to 3) or HPr2 (lanes 4 to 6) was incubated in buffer P with 1 μg of $EIIA^{NAG}$ (A) or the EIIA domain of FruA (S110D) (B) in the presence or absence of 1 mM PEP. After SDS-PAGE, the degree of EIIA phosphorylation was analyzed using ImageJ software as described in "Materials and methods".

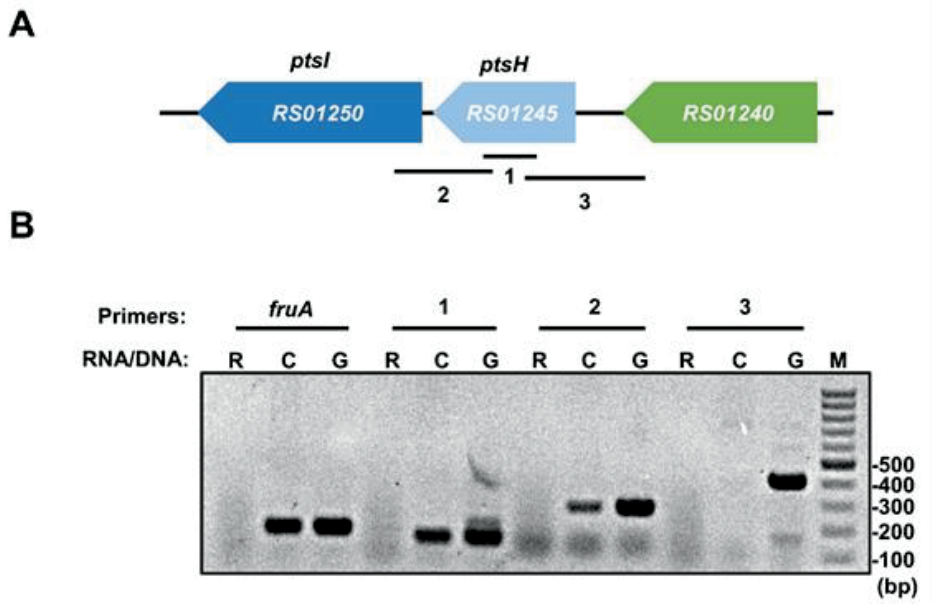

Figure 11. Analysis of co-transcription of *ptsI* (GXM22_RS01250) and *ptsH* (GXM22_RS01245) by RT-PCR

(A) Schematic representation of the genes GXM22_RS01250 (*ptsI*), RS01245 (*ptsH*), and RS01240. The black bars with numbers indicate reverse transcription (RT)-PCR products analyzed in (B). (B) To observe the co-transcription of GXM22_RS01250 (*ptsI*) and RS01245 (*ptsH*), total RNA extracted from *F. prausnitzii* A2-165 grown on fructose was subjected to RT-PCR analysis using specific internal primers as shown in (A) (labeled 1, 2, and 3). RT-PCR products (lanes C) were electrophoresed on 1% agarose gel with the corresponding PCRs without reverse transcriptase (lanes R); PCR products were amplified using genomic DNA (lanes G) to verify primer specificity. PCR products specific for *fruA* were electrophoresed together as a positive control. Lane M refers to the DNA size marker (ThermoFisher Scientific).

Enterococcus faecalis showed that a doubly phosphorylated form of HPr could lead to the phosphorylation of glycerol kinase more efficiently than His-15 phosphorylated HPr (Reizer *et al.*, 1993), postulating that a doubly phosphorylated HPr2 might also function as a phosphoryl donor protein in *F. prausnitzii* to its interacting partners.

2.2 HPr2 may be less efficient in its phosphotransferase activity compared to HPr1

While HPr1 was capable of phosphorylating $EIIA^{NAG}$ almost completely in the presence of PEP and EI, HPr2 was incapable of performing the same as the dephosphorylated $EIIA^{NAG}$ was remaining in noticeable amount after the 2 mins of incubation time. In the same context, while HPr1 fully phosphorylated the fructose-specific EIIA domain, HPr2 could not do so even with the twice amount (Figure 10). Thus, I concluded that HPr1 outcompeted HPr2 in donating the phosphate group to EIIA proteins in terms of efficiency. In support of this hypothesis, I found out that HPr1 is located adjacent to EI, with the possibility of the protein being translated together with EI, as observed in many of the bacteria with PTS. Accordingly, through RT-PCR analysis, I found that EI (encoded by GXM22_RS01250) and HPr1 (encoded by GXM22_RS01245) were co-transcribed as an operon (hereafter referred to as the *ptsHI* operon) in *F. prausnitzii* (Figure 11), consistent with the findings in other bacteria (De Reuse and Danchin, 1988; Gonzy-Tréboul *et al.*, 1989). Hence, it was more likely to assume that HPr2 may be transcribed and expressed independent of the *ptsHI* operon, performing a different role in various circumstances. Due to these reasons, the roles of HPr2 in *F. prausnitzii* remained to

be investigated.

3. Interaction of HPr2 and GalT

3.1 Ligand fishing to find an interacting protein of HPr2

To find the interacting proteins of HPr2, a ligand fishing experiment was performed. *F. prausnitzii* grown on glucose, a sugar source consumed by all *F. prausnitzii* strains tested (Lopez-siles *et al*., 2017), was lysed and the cell lysate was applied to the TALON resins with or without the bait protein HPr2 (Figure 12). After conducting SDS-PAGE, gel excision, and MALDI-TOF mass spectrometry, several binding partners of HPr2 were identified. The α-glucan phosphorylase, HPrK, and aspartate carbamoyltransferase were analyzed to have been interacting with the bait protein, in contrast to the control. Among these, *F. prausnitzii* galactose-1-phosphate uridylyltransferase (GalT) was designated for further analysis, since no such interaction had been reported.

According to the previously published data, galactose is one of the favored carbohydrates of most *F. prausnitzii* strains. Nine out of ten tested strains could metabolize galactose (Lopez-siles *et al*., 2017). The optical density at 600 nm could reach about 0.8 after 24 hours of incubation in YCFA medium supplemented with galactose as the sole carbon source (Lopez-siles *et al*., 2011). Since galactose is one of the major monosaccharides consisting the mucin (Dekker *et al*., 1989), it is reasonable that galactose is highly favored by *F. prausnitzii* that resides in the intestine.

The Leloir pathway of galactose metabolism is a highly conserved metabolism present in eukaryotic organisms such as animals and plants, and also in microbial

cells. When a galactose enters the cell through its transporter, it is converted to galactose 1-phosphate (gal 1-P) by galactose kinase (GalK). Galactose-1-phosphate uridylyltransferase (GalT) then catalyzes the nucleotide exchange between uridine 5'-diphosphate glucose (UDP-glc) and gal 1-P, producing uridine 5'-diphosphate galactose (UDP-gal) and glucose 1-phosphate (glc 1-P) (Figure13A). A close look at the genome of *F. prausnitzii* A2-165 revealed that this strain also possesses the Leloir pathway, metabolizing galactose sequentially through GalK, GalT, and PGM. An RNA-seq data of *F. prausnitzii* A2-165 (Gene Expression Omnibus accession number GSE168352) showed that the genes encoding these proteins were highly expressed only when galactose was supplemented as the sole carbon source (Figure 13B). Since deletion of the gene encoding GalT led to a severe growth defect in *E. coli* while complementation with a *galT*-like gene in a plasmid to the *galT* deletion mutant led to a rescue of the defect (Barreto *et al*., 2005), it was clear that GalT would be an important enzyme essential for the catabolism of galactose.

3.2 Only HPr2, not HPr1, binds to GalT

To confirm the binding of HPr2 and GalT, GalT of *F. prausnitzii* was cloned, overexpressed, and purified in *E. coli*. As in the ligand fishing experiment, histidine-tagged HPr2 was applied to the TALON resin as the bait protein. An increasing amount of HPr2 was applied to the same amount of TALON resin to visualize the concentration-dependent binding of GalT overexpressed in *E. coli*. The HPr1 was applied to the TALON resin in an identical amount as a control protein. Overall, samples with HPr1 and HPr2 as bait proteins or without any bait proteins were prepared, and the cell crude over-expressing GalT was applied. After several steps

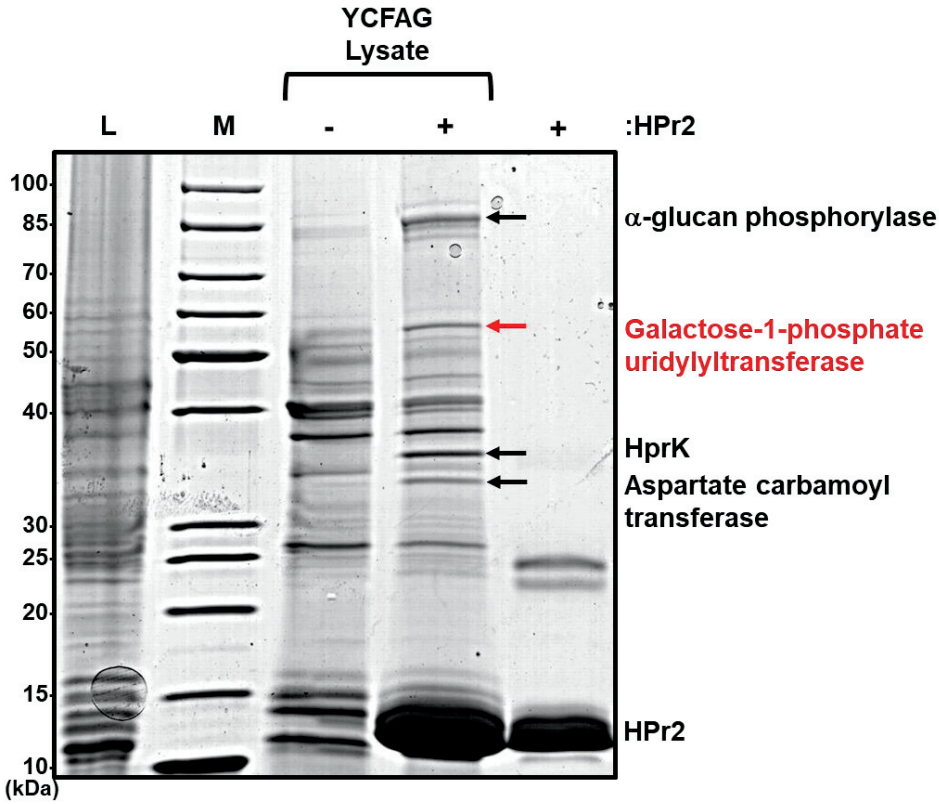

Figure 12. Interaction of HPr2 and proteins in the *F. prausnitzii* cell lysate

A ligand fishing experiment was carried out to search for proteins(s) specifically interacting with HPr2. Crude extract prepared from *F. prausnitzii* grown on YCFA medium supplemented with glucose (YCFAG lysate) was mixed with ('+' lane) or without ('-' lane) 200 μg of purified histidine-tagged HPr2. Each mixture was incubated with 30 μg of TALON resin for metal affinity chromatography. Prot eins bound to each column were analyzed by SDS-PAGE using 4 to 20% g radient gel (KOMA Biotech). Protein bands bound specifically to His-HPr2 a re indicated by arrows. M; protein size marker, L; cell lysate.

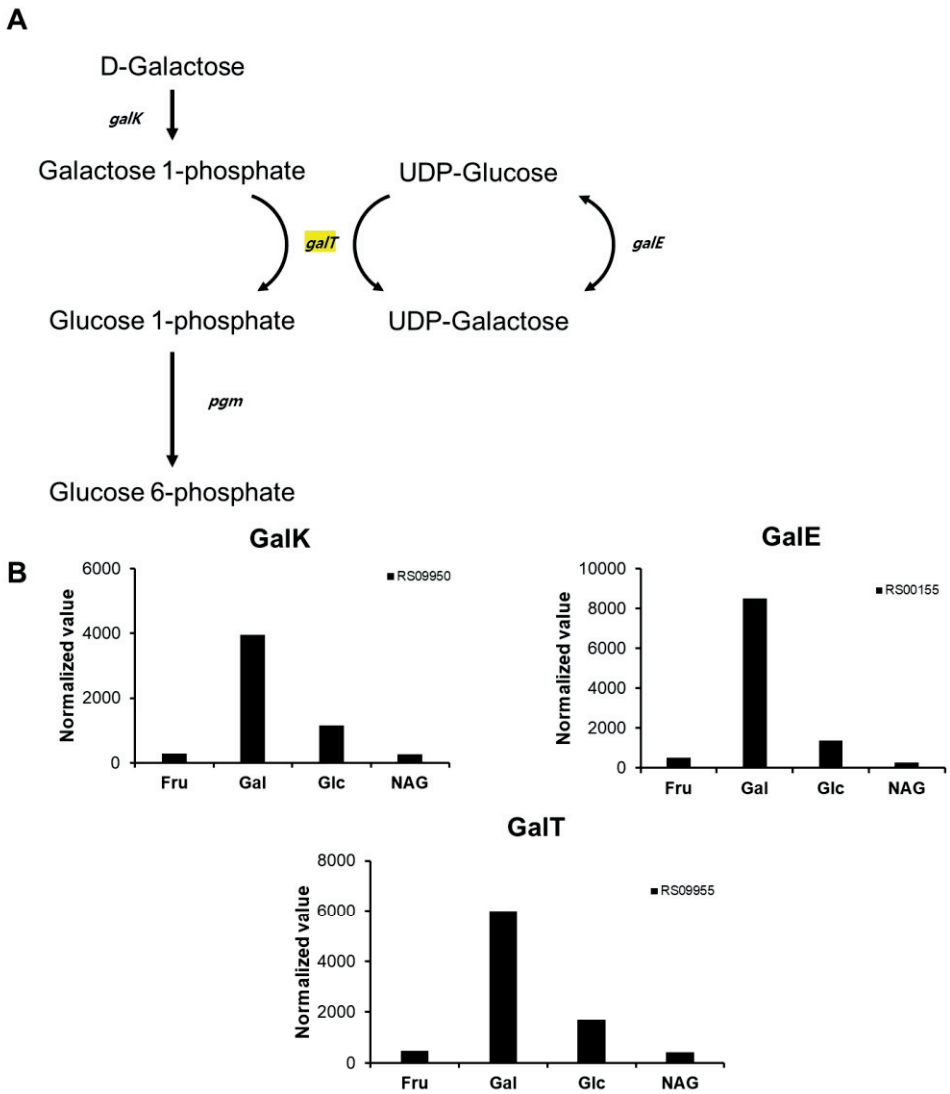

Figure 13. *F. prausnitzii* A2-165 possesses the Leloir pathway

(A) Catabolic Leloir pathway of D-galactose when galactose enters a cell. (B) Relative expressions of the genes consisting the Leloir pathway in *F. prausnitzii* A2-165. Y-axis accounts for raw data normalized through De-seq (Love *et al*., 2014). GalK; galactose kinase, GalT; galactose-1-phosphate uridylyltransferase, GalE; UDP-galactose epimerase, PGM; phosphoglucomutase.

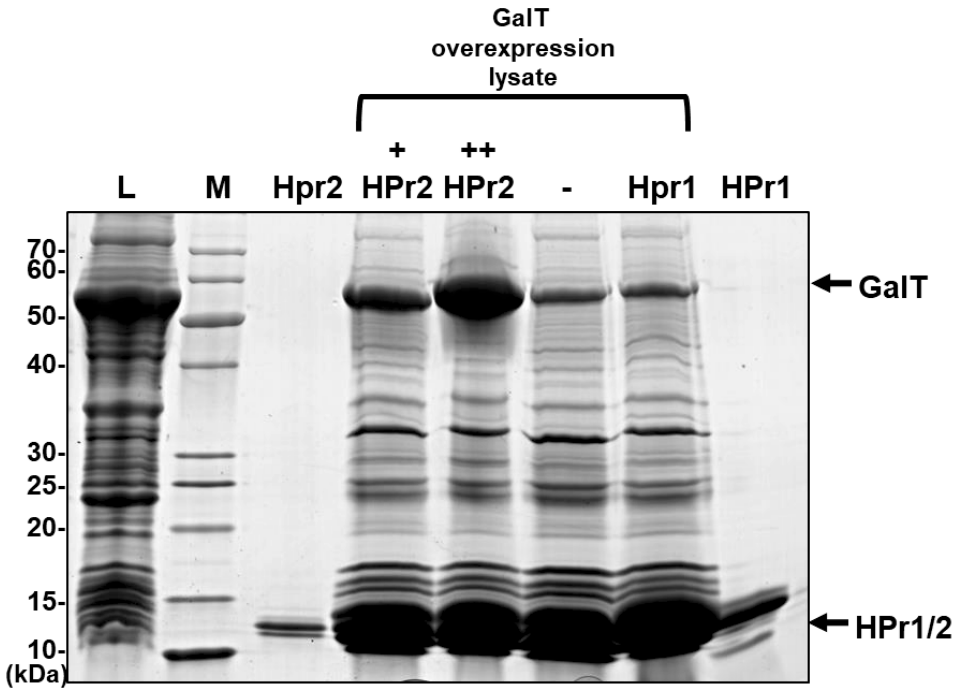

Figure 14. Direct interaction of HPr2 and GalT

GalT was expressed in *E. coli*, and crude extracts were mixed with two different amounts of purified Histidine-tagged HPr2 (0 μg, 50 μg and 140 μg) or HPr1 (50 μg). Each mixture was incubated with 30 μg of TALON resin for metal affinity chromatography. Bound proteins were eluted with 50 μl of 2X SDS sample buffer and analyzed by SDS-PAGE and Coomassie Brilliant Blue staining. Purified HPr2 and Hpr1 were run as controls.

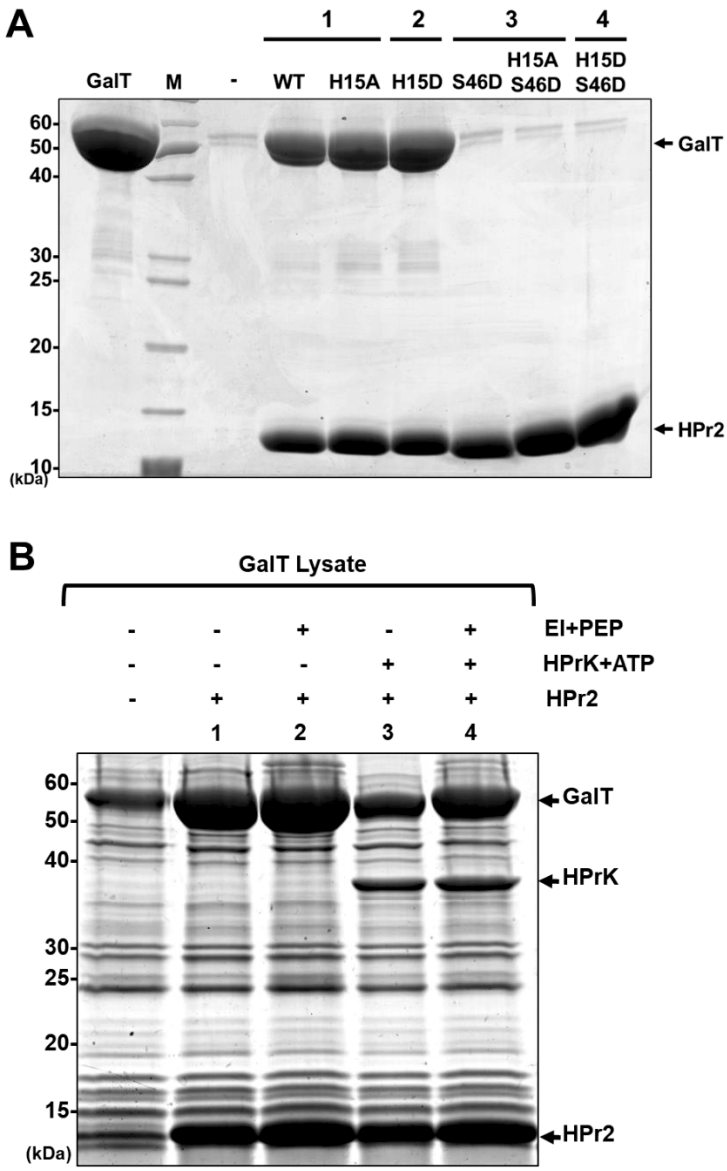

Figure 15. GalT does not interact with serine-phosphorylated HPr2

(A) Purified GalT (100 μg) was mixed with various mutant forms of His-HPr2 (120 μg) as indicated. Each mixture was incubated with 15 μg of TALON resin for metal affinity chromatography. 1; dephosphorylated mimic of HPr2, 2; His-P mimic of HPr2, 3; Ser-P mimic of HPr2, 4; His-P and Ser-P mimic of HPr2, M; marker lane with molecular mass marker proteins (Thermofisher). (B) GalT was over-expressed in *E. coli*, and crude extracts were mixed with purified His-HPr2 (120 μg) in the presence of EI (10 μg) and PEP (2.5 mM), or HPrK (10 μg) and ATP (2.5 mM), all four, or none. Each mixture was subjected to analysis as in (A).

of washing with a mild concentration of imidazole, lysates applied to the TALON resins were eluted, analyzed by SDS-PAGE, and subjected to Coomassie Brilliant Blue staining. The result showed that GalT had indeed interacted with Hpr2 in a concentration-dependent manner (Figure 14). GalT was also eluted out in samples without any bait protein or with HPr1, but the amount of GalT bound to the resin was much lower than the sample with HPr2.

3.3 GalT does not bind to the serine-phosphorylated form of HPr2

The HPr2 of *F. prausnitzii* possesses many forms of phosphorylation: His-P, Ser-P, and His-P/Ser-P. To specify which phosphorylated forms of HPr2 bind to GalT, mutant forms of HPr2 were constructed; to mimic HPr2 (His-P) and HPr2 (Ser-P), the His-15 and Ser-46 residues were substituted with aspartate, respectively annotated as H15D and S46D. The unphosphorylated mimic of HPr2 was constructed by substituting His-15 with Ala, annotated as H15A. Overall, a total of 6 different mutants of HPr2 representing various forms of phosphorylated HPr2 were purified, bound to the TALON resins, and mixed with purified non-tag GalT as in the ligand fishing experiment. Co-elution and SDS-PAGE analysis of each sample revealed that GalT could not bind to the HPr2s with Ser-P mimics (Figure 15A). Whereas GalT was co-eluted with dephosphorylated or histidine-phosphorylated HPr2 mutants, the same could not be observed with HPr2 mutants mimicking serine-phosphorylation and the control sample without any HPr2 bait protein.

The result was repeated with native forms of HPr2 phosphorylated in various forms by the addition of PEP, ATP, HPrK, and EI, as indicated (Figure 15B). In this experiment, histidine-tagged HPr2 was incubated with PEP, ATP, HPrK, and EI as indicated at 37°C. The incubated samples were applied to an equal amount of

TALON resin and the cell lysates over-expressing GalT were applied next. After co-elution, the amounts of GalT bound to the bait protein were visualized through SDS-PAGE and Coomassie Brilliant Blue staining. The result showed that the smallest amount of GalT had remained in the sample with HPr2 (Ser-P) (Figure 15B, lane 3). Thus, I concluded that GalT and HPr2 interact with each other but not when the HPr2 is phosphorylated at the Ser-46 residue. The reason for such a pattern of interaction and the function of GalT regulated by HPr2 thus remained to be investigated.

4. Characterization of *F. prausnitzii* GalT

In order to characterize GalT, the enzyme was purified and subjected to size-exclusion chromatography with molecular mass size markers. GalT has been extensively studied in *E. coli*, and the enzyme was reported as a dimeric protein with a molecular mass of 80 kDa consisted of two subunits of approximately 40 kDa, each monomers forming an active site (Geeganage *et al*., 2000). The theoretical calculation of the molecular weight of F. prausnitzii GalT based on its amino acid sequence was 56.6 kDa. On SDS-PAGE gel, the N-terminally hexahistidine-tagged from of GalT exhibited an apparent molecular mass of ~55 kDa (Figure 16A). Gel filtration analysis however revealed that the enzyme exists as a complex with a molecular mass of ~138.5 kDa (Figure 16B). The GalT of *F. prausnitzii* seemed to differ from the GalT of *E. coli* since there was no significant protein sequence identity between the two proteins when they were analyzed against each other through BLASTp. Rather, the GalT of *F. prausnitzii* showed significant protein identity against the GalTs of Firmicutes, such as *E. faecalis*.

To see whether GalT can perform the same as well-identified GalT of *E. coli*, an

enzyme assay on GalT activity was performed. As mentioned previously, GalT catalyzes the transfer of the uridine group and phosphate group from UDPG and Gal1P. The activity of GalT can be easily detected through the coupled assay; the produced G1P can be converted to G6P by the addition of phosphoglucomutase (PGM), and G6P can further be converted to 6-phosphogluconolactone by glucose 6-phosphate dehydrogenase (G6PDH). When converting G6P, G6PDH reduces $NADP^+$ to NADPH. The formation of NADPH leads to an increase in absorption at 340 nm (Figure 17A). Hence, up to 3 μg of GalT was added with its two substrates in the presence of the excess amount of G6PDH and PGM, and $NADP^+$. The result showed that GalT could function as expected in the presence of the two substrates (Figure 17B).

To see the effect of HPr2 and GalT interaction *in vitro*, an excess amount of HPr2 was added to the reaction mixture and subjected to the coupled enzyme assay as performed previously (Figure 17). HPr2 was phosphorylated by EI, HPrK/P, or both, in the presence of PEP and ATP as indicated by pre-incubation at 37°C to generate His-P, Ser-P, and His-P/Ser-P forms of HPr2s. However, the addition of HPr2s in its various phosphorylation forms did not engender any changes in the activity of GalT (Figure 18A, left panel). The result was repeated when the phosphorylation mimics of HPr2 mutants were added to the reaction mixtures (Figure 18A, right panel). Therefore, a possibility that the interaction between GalT and HPr2 may affect the activity of HPr2 had to be considered thereafter. The mRNA transcription profile also showed that when the bacterium is consuming galactose, the amount of GalT in the cell may be much greater than the amount of HPr2 (Figure 18B), suggesting the possibility of the hypothesis.

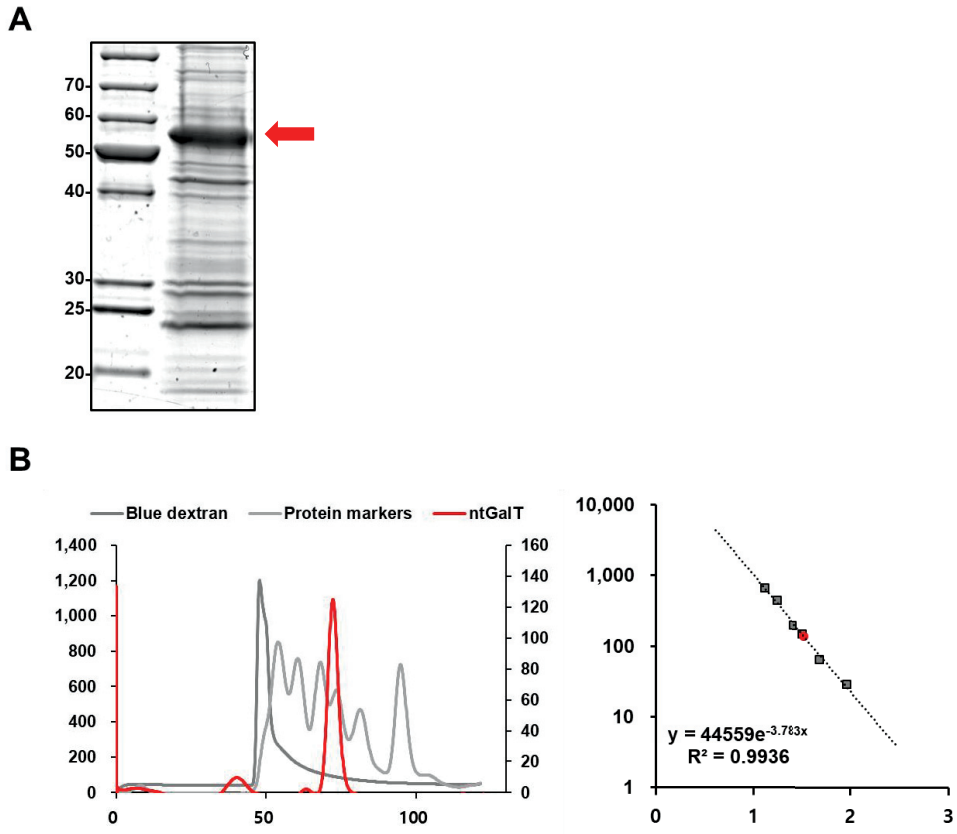

Figure 16. Characterization of GalT

(A) His-tagged GalT was over-expressed in *E. coli* and the cell lysate was analyzed by 4 to 20% gradient SDS-PAGE stained with Coomassie Brilliant Blue. The arrow indicates the protein of interest. (B) Size exclusion chromatography elution profile for measuring the molecular size of GalT (left). The standard curve obtained with proteins from the MWGF1000 Kit (Sigma) (right): Blue dextran (2,000 kDa), Thyroglobulin (669 kDa), Apoferritin (443 kDa), β−amylase (200 kDa), Alcohol dehydrogenase (150 kDa), Albumin (66 kDa), and Carbonic anhydrase (29 kDa). The red spot at ~138 kDa indicates the molecular weight of the protein.

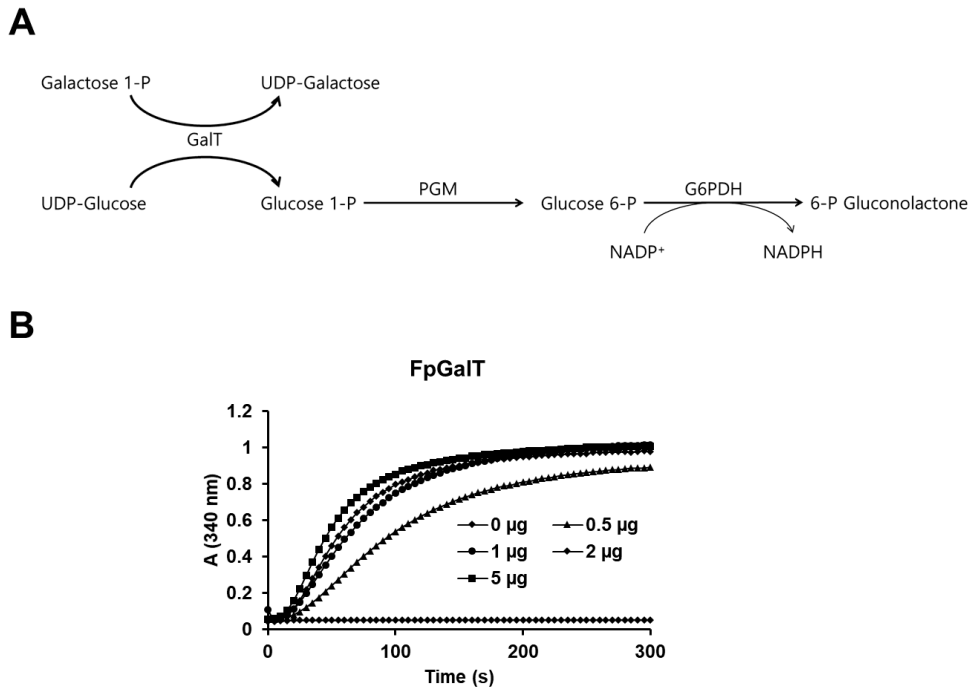

Figure 17. Enzyme assay of GalT

(A) An overall scheme of the spectrophotometric coupled assay to observe the activity of GalT. (B) Enzyme assay of purified GalT was performed using a spectrophotometric coupled assay in buffer E (20 mM Sodium phosphate pH 8.0, 5 mM DTT, 2.5 mM MgCl2, 8 mM Cystein-HCl, 10 µg/ml BSA) by coupling the production of glc 1-P to the reduction of $NADP^+$ in the presence of phosphoglucomutase (PGM) (18.6 µg) and glucose 6-P dehydrogenase (G6PDH) (5 µg). Each mixture was incubated for 5 min at 37°C in the presence of 0.2 mM $NADP^+$, 1 mM UDP-Glc, and the reaction was started by adding 1 mM Gal 1-P to the reaction mixture with the indicated amount of GalT.

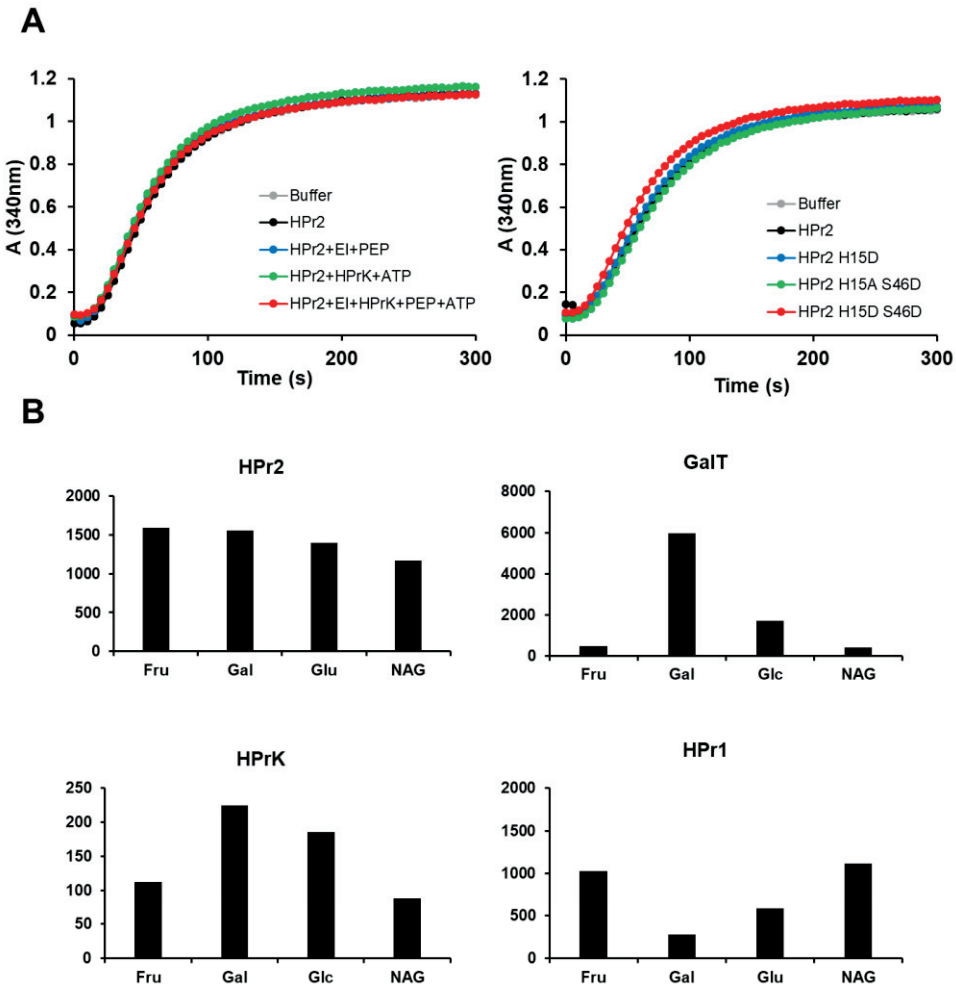

Figure 18. HPr2 has no effect on the activity of GalT

(A) Enzyme assay of purified GalT (5 μg) with the addition of HPr2 (10 μg), EI (1 μg), HPrK (1 μg), PEP (1 mM) and ATP (1 mM) (left panel), and HPr2 mutants (10 μg) (right panel), as indicated in the 'Materials and Methods' section. (B) Relative expressions of the indicated genes in *F. prausnitzii* A2-165. Y-axis accounts for raw data normalized through De-seq (Love *et al*., 2014).

IV. Discussion

The phosphorylation state of PTS proteins reflects the availability of sugars and the consequent physiological state of the cell to the activity of transport proteins, metabolic enzymes, and transcriptional regulators. Such a complex yet plastic regulation provides a significant evolutionary advantage to bacteria (Stülke and Hillen, 1998). On a larger scope, studying PTS proteins is important because the cellular intake of carbohydrates and the subsequent synthesis and secretion of microbial metabolites by such abundant bacteria as *F. prausnitzii* may shape the whole nutrient profile in the large intestine, with a substantial impact exerted on the overall gut microbiota and host cells (Macfarlane, 1998). This study highlights the physiological characteristics of *F. prausnitzii* using biochemical *in vitro* approaches. I have provided an overall model of the PTS in *F. prausnitzii* A2-165 (Figure 2) by reannotating the presumed PTS genes of the bacterium through protein sequence alignment and performing *in vitro* phosphotransferase assays using the membranous protein extracts from *F. prausnitzii* cells grown on diverse carbohydrates and the purified PTS proteins.

Following the investigation on EI and HPr, I assessed the functionality of all EII complexes; while FruA ($EIIABC^{Fru}$) and NagE ($EIICB^{NAG}$) were expressed as functional forms, the remaining three EII complexes appeared to be non-functional in *F. prausnitzii* A2-165. I found that the gene coding for the putative 1-phosphofructokinase (*fruK*), which converts fructose 1-phosphate into fructose 1, 6-

bisphosphate, is adjacent to the gene encoding EIIABC^{Fru}. Additionally, I found that a transcriptional regulator with ~40% protein sequence identity with the *B. subtilis* 168 fructose repressor FruR is also encoded adjacent to *fruK*. The presence of the fructose-specific PTS and fructose metabolic enzymes in *F. prausnitzii* may explain why the supplementation of fructo-oligosaccharides or inulin in diets has led to increased *F. prausnitzii* abundance in patients with obesity and irritable bowel syndrome (Clavel *et al.*, 2005; Dewulf *et al.*, 2013; Hustoft *et al.*, 2017), implying the significance of FruA for the prevalence of *F. prausnitzii* in the gut over other species. It has also been reported that extra dietary fructose can nourish gut microbes that produce short-chain fatty acids (Jang *et al.*, 2018). Therefore, it is also likely that the presence of *F. prausnitzii* possessing FruA in the gut may confer a major benefit to the host's health.

Since the outer layer of vertebrate mucin consists of various complex carbohydrates and glycans that are mostly rich in the amino sugar NAG (Dekker *et al.*, 1991; Wlodarska *et al.*, 2017), efficient transportation of NAG into the cell through the PTS would be advantageous to bacteria residing in the gut. Similar to the fructose-metabolizing gene cluster, genes encoding *N*-acetylglucosamine 6-phosphate deacetylase and glucosamine 6-phosphate deaminase required to utilize this amino sugar are adjacent to *nagE*. As the gene encoding NAG-specific PTS (PTS^{NAG}) has been reported as one of the most abundant transporter genes encoded in the commensal Clostridiales order (Wlodarska *et al.*, 2017), it can be assumed that *F. prausnitzii*, which belongs to it, actively metabolizes NAG through PTS in the gut.

Despite the presence of putative genes encoding membrane PTS proteins specific for glucose, mannose, and maltose (Table 1), the transcription levels of these genes could only barely be detected and their functionalities were not observed through our

methods (Figures 7 and 8). Interestingly, although glucose is utilized by most strains of *F. prausnitzii* (Duncan *et al.*, 2002; Heinken *et al.*, 2014), it appears to be transported by mechanisms other than the PTS in *F. prausnitzii* A2-165 (Figure 8). Since glucose from the diet is readily absorbed by the host epithelial cells as well as other bacteria in the small intestine (Utzschneider *et al.*, 2016; Woting and Blaut, 2016), it is a relatively scarce nutrient in the distal colon, where *F. prausnitzii* resides (Duncan *et al.*, 2009; Lopez-Siles *et al.*, 2016). Intriguingly, *Bifidobacterium bifidum* MB245 and *Bifidobacterium lactis* DSM10140, the common anaerobes also residing in large intestines of animals, only harbor the fructose-specific PTS, consuming glucose only through facilitated diffusion (Barabote and Saier, 2005; Briczinski *et al.*, 2008). As one of the most common constituents of dietary probiotics, they successfully colonize the large intestine even after belated introduction (Bartosch *et al.*, 2005), implying that possession of the fructose and NAG PTS rather than the glucose PTS may confer some selective advantage for the bacteria to compete against other species in the gut (Briczinski *et al.*, 2008).

The functional dissection of the PTS of *F. prausnitzii* has revealed that the system may be more of a regulatory pathway of cell physiologies, than a transporting mechanism for carbohydrates. Among the PTS components, the general component HPr2 was chosen as the protein of interest due to its capability in taking various phosphorylation forms, and its lack of phosphotransferase activity in contrast to HPr1. The ligand fishing experiment with HPr2 revealed several interacting proteins of HPr2, and among these, GalT, an enzyme of the Leloir pathway, was chosen for investigation. Since GalT is known as an essential protein when a cell is consuming galactose (Barreto *et al.*, 2005), investigation on the interaction and its influence may be an important concern and suggests a deeper exploration.

In summary, the major focus of previous studies on *F. prausnitzii* was on explaining the negative correlation between the bacterial abundance and occurrence or severity of the related diseases in terms of their secreted substances. However, to understand the mechanisms of their prevalence in the gut, it is necessary to determine the nutrients used by *F. prausnitzii* and their effect on the survival of the species. The PTS is a widely distributed and highly efficient carbohydrate transport system found in most bacterial species that catalyzes the simultaneous phosphorylation and import of cognate sugars; the phosphorylation state of PTS proteins reflects the availability of sugars and the consequent physiological state of the cell to the activity of transport proteins, metabolic enzymes, and transcriptional regulators (Stülke and Hillen, 1998). Hence, identification of the functional PTS components and their interacting partners in *F. prausnitzii* A2-165 may be important in explaining how this seemingly beneficial microbe can adapt and thrive competitively in the guts of healthy humans. Such investigation may also provide methods to preserve this extremely oxygen-sensitive anaerobe in the gut, further offering clues on the same for several beneficial Firmicutes.

V. References

Alpert, C.A., Frank, R., Stüber, K., Deutscher, J., and Hengstenberg, W. (1985) Phosphoenolpyruvate-dependent protein kinase enzyme I of *Streptococcus faecalis*: purification and properties of the enzyme and characterization of its active center. *Biochemistry* **24**: 959-964.

Arumugam, M., Raes, J., Pelletier, E., Le Paslier, D., Yamada, T., Mende, D.R. *et al.* (2011) Enterotypes of the human gut microbiome. *Nature* **473**: 174-180.

Barabote, R.D., and Saier, M.H. (2005) Comparative genomic analyses of the bacterial phosphotransferase system. *Microbiol Mol Biol Rev* **69**: 608-634.

Barreto, M., Jedlicki, E., and Holmes, D.S. (2005) Identification of a gene cluster for the formation of extracellular polysaccharide precursors in the chemolithoautotroph *Acidithiobacillus ferrooxidans*. *Appl Environ Microbiol* **71**: 2902-2909.

Bartosch, S., Woodmansey, E.J., Paterson, J.C., McMurdo, M.E., and Macfarlane, G.T. (2005) Microbiological effects of consuming a synbiotic containing *Bifidobacterium bifidum*, *Bifidobacterium lactis*, and oligofructose in elderly persons, determined by real-time polymerase chain reaction and counting of viable bacteria. *Clin Infect Dis* **40**: 28-37.

Bolger, A.M., Lohse, M., and Usadel, B. (2014) Trimmomatic: a flexible trimmer for Illumina sequence data. *Bioinformatics* **30**: 2114-2120.

Breyner, N.M., Michon, C., de Sousa, C.S., Vilas Boas, P.B., Chain, F., Azevedo, V.A. *et al.* (2017) Microbial Anti-Inflammatory Molecule (MAM) from *Faecalibacterium prausnitzii* Shows a Protective Effect on DNBS and DSS-Induced Colitis Model in Mice through Inhibition of NF-κB Pathway. *Front Microbiol* **8**: 114.

Briczinski, E.P., Phillips, A.T., and Roberts, R.F. (2008) Transport of glucose by *Bifidobacterium animalis* subsp. *lactis* occurs via facilitated diffusion. *Appl Environ Microbiol* **74**: 6941-6948.

Cao, Y., Shen, J., and Ran, Z.H. (2014) Association between *Faecalibacterium prausnitzii* Reduction and Inflammatory Bowel Disease: A Meta-Analysis and Systematic Review of the Literature. *Gastroenterol Res Pract* **2014**: 872725.

Choe, M., Park, Y.H., Lee, C.R., Kim, Y.R., and Seok, Y.J. (2017) The general PTS component HPr determines the preference for glucose over mannitol. *Sci Rep* **7**: 43431.

Clavel, T., Fallani, M., Lepage, P., Levenez, F., Mathey, J., Rochet, V. *et al.* (2005) Isoflavones and functional foods alter the dominant intestinal microbiota in postmenopausal women. *J Nutr* **135**: 2786-2792.

De Reuse, H., and Danchin, A. (1988) The *ptsH*, *ptsI*, and *crr* genes of the *Escherichia coli* phosphoenolpyruvate-dependent phosphotransferase system: a complex operon with several modes of transcription. *J Bacteriol* **170**: 3827-3837.

Dekker, J., Van Beurden-Lamers, W.M., Oprins, A., and Strous, G.J. (1989). Isolation and structural analysis of rat gastric mucus glycoprotein suggests a homogeneous protein backbone. Biochem J *260*, 717-723.

Dekker, J., Aelmans, P.H., and Strous, G.J. (1991) The oligomeric structure of rat and human gastric mucins. *Biochem J* **277 (Pt 2)**: 423-427.

Deutscher, J., Francke, C., and Postma, P.W. (2006) How phosphotransferase system-related protein phosphorylation regulates carbohydrate metabolism in bacteria. *Microbiol Mol Biol Rev* **70**: 939-1031.

Deutscher, J., Aké, F.M., Derkaoui, M., Zébré, A.C., Cao, T.N., Bouraoui, H. *et al.* (2014) The bacterial phosphoenolpyruvate:carbohydrate phosphotransferase system: regulation by protein phosphorylation and phosphorylation-dependent protein-protein interactions. *Microbiol Mol Biol Rev* **78**: 231-256.

Dewulf, E.M., Cani, P.D., Claus, S.P., Fuentes, S., Puylaert, P.G., Neyrinck, A.M. *et al.* (2013) Insight into the prebiotic concept: lessons from an exploratory, double blind intervention study with inulin-type fructans in obese women. *Gut* **62**: 1112-1121.

Dörschug, M., Frank, R., Kalbitzer, H.R., Hengstenberg, W., and Deutscher, J. (1984) Phosphoenolpyruvate-dependent phosphorylation site in enzyme III^{glc} of the *Escherichia coli* phosphotransferase system. *Eur J Biochem* **144**: 113-119.

Duncan, S.H., Louis, P., Thomson, J.M., and Flint, H.J. (2009) The role of pH in determining the species composition of the human colonic microbiota. *Environ Microbiol* **11**: 2112-2122.

Duncan, S.H., Hold, G.L., Harmsen, H.J.M., Stewart, C.S., and Flint, H.J. (2002) Growth requirements and fermentation products of *Fusobacterium prausnitzii*, and a proposal to reclassify it as *Faecalibacterium prausnitzii* gen. nov., comb. nov. *Int J Syst Evol Microbiol* **52**: 2141-2146.

Duncan, S.H., Scott, K.P., Ramsay, A.G., Harmsen, H.J., Welling, G.W., Stewart, C.S., and Flint, H.J. (2003) Effects of alternative dietary substrates on competition between human colonic bacteria in an anaerobic fermentor system. *Appl Environ Microbiol* **69**: 1136-1142.

El-Semman, I.E., Karlsson, F.H., Shoaie, S., Nookaew, I., Soliman, T.H., and Nielsen, J. (2014) Genome-scale metabolic reconstructions of *Bifidobacterium adolescentis* L2-32 and *Faecalibacterium prausnitzii* A2-165 and their interaction. *BMC Syst Biol* **8**: 41.

Fieulaine, S., Morera, S., Poncet, S., Mijakovic, I., Galinier, A., Janin, J. *et al.* (2002) X-ray structure of a bifunctional protein kinase in complex with its protein substrate HPr. *Proc Natl Acad Sci U S A* **99**: 13437-13441.

Fitzgerald, C.B., Shkoporov, A.N., Sutton, T.D.S., Chaplin, A.V., Velayudhan, V., Ross, R.P., and Hill, C. (2018) Comparative analysis of *Faecalibacterium prausnitzii* genomes shows a high level of genome plasticity and warrants separation into new species-level taxa. *BMC Genomics* **19**: 931.

Flint, H.J., Scott, K.P., Louis, P., and Duncan, S.H. (2012) The role of the gut microbiota in nutrition and health. *Nat Rev Gastroenterol Hepatol* **9**: 577-589.

Gassner, M., Stehlik, D., Schrecker, O., Hengstenberg, W., Maurer, W., and Rüterjans, H. (1977) The phosphoenolpyruvate-dependent phosphotransferase system of *Staphylococcus aureus*. 2. ^{1}H and ^{31}P-nuclear-magnetic-resonance studies on the phosphocarrier protein HPr, phosphohistidines and phosphorylated HPr. *Eur J Biochem* **75**: 287-296.

Geeganage, S., Ling, V.W., and Frey, P.A. (2000) Roles of two conserved amino acid residues in the active site of galactose-1-phosphate uridylyltransferase: an essential serine and a nonessential cysteine. *Biochemistry* **39**: 5397-5404.

Gonzy-Tréboul, G., Zagorec, M., Rain-Guion, M.C., and Steinmetz, M. (1989) Phosphoenolpyruvate:sugar phosphotransferase system of *Bacillus subtilis*: nucleotide sequence of *ptsX*, *ptsH* and the 5'-end of *ptsI* and evidence for a *ptsHI* operon. *Mol Microbiol* **3**: 103-112.

Gurung, M., Li, Z., You, H., Rodrigues, R., Jump, D.B., Morgun, A., and Shulzhenko, N. (2020) Role of gut microbiota in type 2 diabetes pathophysiology. *EBioMedicine* **51**: 102590.

Guo, P., Zhang, K., Ma, X., and He, P. (2020) *Clostridium* species as probiotics: potentials and challenges. *J Anim Sci Biotechnol* **11**: 24.

Halbedel, S., and Stülke, J. (2005) Dual phosphorylation of *Mycoplasma pneumoniae* HPr by Enzyme I and HPr kinase suggests an extended phosphoryl group susceptibility of HPr. *FEMS Microbiol Lett* **247**: 193-198.

Ham, H. (2019) Characterization of the PTS in the beneficial human gut bacterium *Faecalibacterium prausnitzii* A2-165. [Master's dissertation]. Seoul National University, Seoul, Republic of Korea

Hayes, C.A., Dalia, T.N., and Dalia, A.B. (2017) Systematic genetic dissection of PTS in *Vibrio cholerae* uncovers a novel glucose transporter and a limited role for PTS during infection of a mammalian host. *Mol Microbiol* **104**: 568-579.

Heinken, A., Khan, M.T., Paglia, G., Rodionov, D.A., Harmsen, H.J., and Thiele, I. (2014) Functional metabolic map of *Faecalibacterium prausnitzii*, a beneficial human gut microbe. *J Bacteriol* **196**: 3289-3302.

Heo, K., Park, Y.H., Lee, K.A., Kim, J., Ham, H.I., Kim, B.G. *et al.* (2019) Sugar-mediated regulation of a c-di-GMP phosphodiesterase in *Vibrio cholerae*. *Nat Commun* **10**: 5358.

Hogema, B.M., Arents, J.C., Bader, R., Eijkemans, K., Yoshida, H., Takahashi, H. *et al.* (1998) Inducer exclusion in *Escherichia coli* by non-PTS substrates: the role of the PEP to pyruvate ratio in determining the phosphorylation state of enzyme IIA^{Glc}. *Mol Microbiol* **30**: 487-498.

Hustoft, T.N., Hausken, T., Ystad, S.O., Valeur, J., Brokstad, K., Hatlebakk, J.G., and Lied, G.A. (2017) Effects of varying dietary content of fermentable short-chain carbohydrates on symptoms, fecal microenvironment, and cytokine profiles in patients with irritable bowel syndrome. *Neurogastroenterol Motil* **29**.

Jang, C., Hui, S., Lu, W., Cowan, A.J., Morscher, R.J., Lee, G. *et al.* (2018) The Small Intestine Converts Dietary Fructose into Glucose and Organic Acids. *Cell Metab* **27**: 351-361 e353.

Khan, M.T., Duncan, S.H., Stams, A.J., van Dijl, J.M., Flint, H.J., and Harmsen, H.J. (2012) The gut anaerobe *Faecalibacterium prausnitzii* uses an extracellular electron shuttle to grow at oxic-anoxic interphases. *ISME J* **6**: 1578-1585.

Kim, D., Paggi, J.M., Park, C., Bennett, C., and Salzberg, S.L. (2019) Graph-based genome alignment and genotyping with HISAT2 and HISAT-genotype. *Nat Biotechnol* **37**: 907-915.

Kim, E.J., Cho, Y.J., Chung, W.H., and Roe, J.H. (2020) The role of Rsv1 in the transcriptional regulation of genes involved in sugar metabolism for long-term survival. *FEBS J* **287**: 878-896.

Kim, H.M., Park, Y.H., Yoon, C.K., and Seok, Y.J. (2015) Histidine phosphocarrier protein regulates pyruvate kinase A activity in response to glucose in *Vibrio vulnificus*. *Mol Microbiol* **96**: 293-305.

Kotrba, P., Inui, M., and Yukawa, H. (2001) Bacterial phosphotransferase system (PTS) in carbohydrate uptake and control of carbon metabolism. *J Biosci Bioeng* **92**: 502-517.

Lee, C.R., Park, Y.H., Min, H., Kim, Y.R., and Seok, Y.J. (2019) Determination of protein phosphorylation by polyacrylamide gel electrophoresis. *J Microbiol* **57**: 93-100.

Leloir, L.F. (1971) Two decades of research on the biosynthesis of saccharides. *Science* **172**: 1299-1303.

Lemaire, H.G., and Muller-Hill, B. (1986) Nucleotide sequences of the *gal E* gene and the

gal T gene of *E. coli*. *Nucleic Acids Res* **14**: 7705-7711.

Liao, Y., Smyth, G.K., and Shi, W. (2014) featureCounts: an efficient general purpose program for assigning sequence reads to genomic features. *Bioinformatics* **30**: 923-930.

Lopez-Siles, M., Khan, T.M., Duncan, S.H., Harmsen, H.J., Garcia-Gil, L.J., and Flint, H.J. (2012) Cultured representatives of two major phylogroups of human colonic *Faecalibacterium prausnitzii* can utilize pectin, uronic acids, and host-

derived substrates for growth. *Appl Environ Microbiol* **78**: 420-428.

Lopez-Siles, M., Martinez-Medina, M., Surís-Valls, R., Aldeguer, X., Sabat-Mir, M., Duncan, S.H. *et al.* (2016) Changes in the Abundance of *Faecalibacterium prausnitzii* Phylogroups I and II in the Intestinal Mucosa of Inflammatory Bowel Disease and Patients with Colorectal Cancer. *Inflamm Bowel Dis* **22**: 28-41.

Love, M.I., Huber, W., and Anders, S. (2014) Moderated estimation of fold change and dispersion for RNA-seq data with DESeq2. *Genome Biol* **15**: 550.

Macfarlane, S.Q., M.E.; Hopkins, M.J.; Newton, D.F.; Macfarlane, G.T. (1998) Polysaccharide degradation by human intestinal bacteria during growth under multi-substrate limiting conditions in a three-stage continuous culture system. *FEMS Microbiol Ecol* **26**: 231-243.

Martín, R., Miquel, S., Benevides, L., Bridonneau, C., Robert, V., Hudault, S. *et al.* (2017) Functional Characterization of Novel *Faecalibacterium prausnitzii* Strains Isolated from Healthy Volunteers: A Step Forward in the Use of *F. prausnitzii* as a Next-Generation Probiotic. *Front Microbiol* **8**: 1226.

Mijakovic, I., Poncet, S., Galinier, A., Monedero, V., Fieulaine, S., Janin, J. *et al.* (2002) Pyrophosphate-producing protein dephosphorylation by HPr kinase/phosphorylase: a relic of early life? *Proc Natl Acad Sci U S A* **99**: 13442-13447.

Miquel, S., Martín, R., Bridonneau, C., Robert, V., Sokol, H., Bermúdez-Humarán, L.G. *et al.* (2014) Ecology and metabolism of the beneficial intestinal commensal bacterium *Faecalibacterium prausnitzii*. *Gut Microbes* **5**: 146-151.

Miquel, S., Martín, R., Rossi, O., Bermúdez-Humarán, L.G., Chatel, J.M., Sokol, H. *et al.* (2013) *Faecalibacterium prausnitzii* and human intestinal health. *Curr Opin Microbiol* **16**: 255-261.

Miquel, S., Leclerc, M., Martin, R., Chain, F., Lenoir, M., Raguideau, S. et al. (2015) Identification of metabolic signatures linked to anti-inflammatory effects of *Faecalibacterium prausnitzii*. *mBio* **6**.

Park, S., Park, Y.H., Lee, C.R., Kim, Y.R., and Seok, Y.J. (2016) Glucose induces delocalization of a flagellar biosynthesis protein from the flagellated pole. *Mol Microbiol* **101**: 795-808.

Park, Y.H., Lee, C.R., Choe, M., and Seok, Y.J. (2013) HPr antagonizes the anti-sigma70 activity of Rsd in *Escherichia coli*. *Proc Natl Acad Sci U S A* **110**: 21142-21147.

Plumbridge, J. (2001) Regulation of PTS gene expression by the homologous transcriptional regulators, Mlc and NagC, in *Escherichia coli* (or how two similar repressors can behave differently). *J Mol Microbiol Biotechnol* **3**: 371-380.

Poncet, S., Soret, M., Mervelet, P., Deutscher, J., and Noirot, P. (2009) Transcriptional activator YesS is stimulated by histidine-phosphorylated HPr of the *Bacillus subtilis* phosphotransferase system. *J Biol Chem* **284**: 28188-28197.

Reizer, J., Romano, A.H., and Deutscher, J. (1993) The role of phosphorylation of HPr, a phosphocarrier protein of the phosphotransferase system, in the regulation of carbon metabolism in gram-positive bacteria. *J Cell Biochem* **51**: 19-24.

Reizer, J., Reizer, A., and Saier, M.H., Jr. (1995) Novel phosphotransferase system genes revealed by bacterial genome analysis--a gene cluster encoding a unique Enzyme I and the proteins of a fructose-like permease system. *Microbiology (Reading)* **141 (Pt 4)**: 961-971.

Reizer, J., Novotny, M.J., Panos, C., and Saier, M.H., Jr. (1983) Mechanism of inducer expulsion in *Streptococcus pyogenes*: a two-step process activated by ATP. *J Bacteriol* **156**: 354-361.

Reizer, J., Bachem, S., Reizer, A., Arnaud, M., Saier, M.H., Jr., and Stülke, J. (1999) Novel phosphotransferase system genes revealed by genome analysis - the complete complement of PTS proteins encoded within the genome of *Bacillus subtilis*. *Microbiology (Reading)* **145 (Pt 12)**: 3419-3429.

Singh, K.D., Schmalisch, M.H., Stülke, J., and Görke, B. (2008) Carbon catabolite repression in *Bacillus subtilis*: quantitative analysis of repression exerted by different carbon sources. *J Bacteriol* **190**: 7275-7284.

Sokol, H., Pigneur, B., Watterlot, L., Lakhdari, O., Bermúdez-Humarán, L.G., Gratadoux, J.J. *et al.* (2008) *Faecalibacterium prausnitzii* is an anti-inflammatory commensal bacterium identified by gut microbiota analysis of Crohn disease patients. *Proc Natl Acad Sci U S A* **105**: 16731-16736.

Stülke, J., and Hillen, W. (1998) Coupling physiology and gene regulation in bacteria: the phosphotransferase sugar uptake system delivers the signals.

Naturwissenschaften **85**: 583-592.

Tremaroli, V., and Backhed, F. (2012) Functional interactions between the gut microbiota and host metabolism. *Nature* **489**: 242-249.

Utzschneider, K.M., Kratz, M., Damman, C.J., and Hullar, M. (2016) Mechanisms Linking the Gut Microbiome and Glucose Metabolism. *J Clin Endocrinol Metab* **101**: 1445-1454.

Wang, G., Sondej, M., Garrett, D.S., Peterkofsky, A., and Clore, G.M. (2000) A common interface on histidine-containing phosphocarrier protein for interaction with its partner proteins. *J Biol Chem* **275**: 16401-16403.

Wlodarska, M., Luo, C., Kolde, R., d'Hennezel, E., Annand, J.W., Heim, C.E. *et al.* (2017) Indoleacrylic Acid Produced by Commensal Peptostreptococcus Species Suppresses Inflammation. *Cell Host Microbe* **22**: 25-37 e26.

Woting, A., and Blaut, M. (2016) The Intestinal Microbiota in Metabolic Disease. *Nutrients* **8**: 202.

Yoon, C.K., Kang, D., Kim, M.K., and Seok, Y.J. (2021) *Vibrio cholerae* FruR facilitates binding of RNA polymerase to the *fru* promoter in the presence of fructose 1-phosphate. *Nucleic Acids Res* **49**: 1397–1410.

Zoetendal, E.G., Rajilic-Stojanovic, M., and de Vos, W.M. (2008) High-throughput diversity and functionality analysis of the gastrointestinal tract microbiota. *Gut* **57**: 1605-1615.

국문 초록

피칼리박테리움 프로스니치는 건강한 성인 장내 미생물군 (microbiota) 중의 우점종으로, 항염증 물질을 생산할 수 있는 능력이 있어 유익균으로 여겨지고 있다. 그러나 피칼리박테리움 프로스니치가 장 내의 양분을 어떻게 섭취하여 장내에서 우세하게 생존할 수 있는지에 관한 연구는 전무한 상태이다. 당 수송 인산전달계 (phosphoenolpyruvate: carbohydrate phosphotransferase system, PTS)는 박테리아가 사용하는 효율적인 당 수송 시스템이다. PTS는 모든 당 수송방식에서 공통으로 사용되는 일반 PTS 단백질인 EI과 HPr, 그리고 당 특이적으로 사용되는 EII 단백질로 구성되어 있다. PEP로부터 유래된 인산기는 EI, HPr, 당 특이적인 EII 단백질들로 순차적으로 전달되고, 마지막으로 장내로 수송되는 당이 인산화된다. PTS는 당 수송뿐만 아니라, 인산화 상태에 따른 단백질 상호작용을 통해 세포 내의 다양한 생리 활성을 조절한다고 알려져 있다. 기존 연구에서, 피칼리박테리움 프로스니치 A2-165균의 PTS는 16개의 단백질로 구성되었으며 특이적으로 두 개의 EI homolog 중에 한 가지만 인산전달기능이 있는 것과 두 개의 HPr중 HPr1은 인산전달계 과정에 중점적으로 참여하는 반면 HPr2는 생리 조절자의 역할을 할 것으로 예상한 바 있다.

본 연구에서는, 피칼리박테리움 프로스니치 A2-165의 당 특이적인

PTS 구성요소들의 기능을 살펴보고자 *in vitro* 인산기전달실험을 수행하였고, 피칼리박테리움 프로스니치에서 추출한 막단백질들을 사용해 연구한 결과 과당과 *N*-아세틸글루코사민이 PTS를 통해 수송된다는 것을 발견하였다. 또한 PTS 단백질의 생리 조절 기능을 연구하는 과정에서 HPr2가 갈락토스 분해 과정에 필수적인 갈락토스 1-인산 유리딜기 전이효소 (galactose-1-phosphate uridylyltransferase)와 상호작용하는 것을 새롭게 발견하였다. 결과적으로, 피칼리박테리움 프로스니치 PTS가 장내에 존재하는 탄수화물을 섭취하는 과정에 관여할 것으로 추측하였고, 이러한 기작이 장내에서 경쟁하고 생존하는데 이바지할 것으로 예상하였다.

주요어:

피칼리박테리움 프로스니치, 장내 세균, 당 수송 인산전달계, 당 특이적 PTS, 갈락토스 1-인산 유리딜기 전이효소, 박테리아 생리

Student Number: 2019-24211